Profiling of aerosol microphysical properties at several EARLINET/AERONET sites during July 2012 ChArMEx/EMEP campaign

M. J. Granados-Muñoz, F. Navas-Guzmán, J. L. Guerrero-Rascado, J. A. Bravo-Aranda, I. Binietoglou, S. N. Pereira, S. Basart, J. M. Baldasano, L. Belegante, A. Chaikovsky, et al.

Atmos. Chem. Phys. Discuss., 15, 32831–32887, 2015
www.atmos-chem-phys-discuss.net/15/32831/2015/
doi:10.5194/acpd-15-32831-2015

Atmospheric Chemistry and Physics Discussions

Profiling of aerosol microphysical properties at several EARLINET/AERONET sites during July 2012 ChArMEx/EMEP campaign

M. J. Granados-Muñoz[1,2,a], F. Navas-Guzmán[3], J. L. Guerrero-Rascado[1,2], J. A. Bravo-Aranda[1,2], I. Binietoglou[4], S. N. Pereira[5], S. Basart[6], J. M. Baldasano[6], L. Belegante[4], A. Chaikovsky[7], A. Comerón[8], G. D'Amico[9], O. Dubovik[10], L. Ilic[11], P. Kokkalis[12], C. Muñoz-Porcar[8], S. Nickovic[11,13], D. Nicolae[4], F. J. Olmo[1,2], A. Papayannis[12], G. Pappalardo[9], A. Rodríguez[8], K. Schepanski[14], M. Sicard[8,15], A. Vukovic[11,16], U. Wandinger[14], F. Dulac[17], and L. Alados-Arboledas[1,2]

[1]Dpt. Applied Physics, Faculty of Sciences, University of Granada, Fuentenueva s/n, 18071, Granada, Spain
[2]Andalusian Institute for Earth System Research (IISTA-CEAMA), Avda. del Mediterráneo s/n, 18006, Granada, Spain
[3]Institute of Applied Physics (IAP), University of Bern, Bern, Switzerland
[4]National Institute of R&D for Optoelectronics, Magurele, Ilfov, Romania

[5]Departamento de Física, ECT, Instituto de Ciências da Terra, IIFA, Universidade de Évora, Évora, Portugal
[6]Earth Sciences Department, Barcelona Supercomputing Center-Centro Nacional de Supercomputación, BSC-CNS, Barcelona, Spain
[7]Institute of Physics, National Academy of Sciences of Belarus, Minsk, Belarus
[8]Dept. of Signal Theory and Communications, Remote Sensing Lab. (RSLab), Universitat Politècnica de Catalunya, Barcelona, Spain
[9]Consiglio Nazionale delle Ricerche – Istituto di Metodologie per l Analisi Ambientale (CNR-IMAA), Potenza, Italy
[10]Laboratoire d'Optique Atmospherique, CNRS Universite de Lille 1, Bat P5 Cite scientifique, 59655, Villeneuve d'Ascq CEDEX, France
[11]Institute of Physics, University of Belgrade, Belgrade, Serbia
[12]National Technical University of Athens, Physics Department, Laser Remote Sensing Laboratory, Zografou, Greece
[13]South East European Virtual Climate Change Center, Republic Hydrometeorological Service, Belgrade, Serbia
[14]Leibniz Institute for Tropospheric Research, Leipzig, Germany
[15]Ciències i Tecnologies de l'Espai – Centre de Recerca de l'Aeronàutica i de l'Espai/Institut d'Estudis Espacials de Catalunya (CTE-CRAE/IEEC), Universitat Politècnica de Catalunya, Barcelona, Spain
[16]Faculty of Agriculture, University of Belgrade, Belgrade, Serbia
[17]Laboratoire des Sciences du Climat et de l'Environnement (IPSL-LSCE), CEA-CNRS-UVSQ, CEA Saclay, Gif-sur-Yvette, France
[a]currently at: Table Mountain Facility, NASA/Jet Propulsion Laboratory, California Institute of Technology, Wrightwood, California, USA

Received: 5 August 2015 – Accepted: 10 November 2015 – Published: 20 November 2015

Correspondence to: M. J. Granados-Muñoz (mjgranados@ugr.es)

Published by Copernicus Publications on behalf of the European Geosciences Union.

ACPD
15, 32831–32887, 2015

Abstract

The analysis of aerosol microphysical properties profiles at different European stations is made in the framework of the ChArMEx/EMEP 2012 field campaign (9–11 July 2012). During and in support to this campaign, five lidar ground-based stations (Athens, Barcelona, Bucharest, Évora and Granada) performed 72 h of continuous lidar and collocated and coincident sun-photometer measurements. Therefore it was possible to retrieve volume concentration profiles with the Lidar Radiometer Inversion Code (LIRIC). Results indicated the presence of a mineral dust plume affecting the Western Mediterranean region (mainly Granada station) whereas a different aerosol plume was observed over the Balkans area. LIRIC profiles showed a predominance of coarse spheroid particles above Granada, as expected for mineral dust, and an aerosol plume composed mainly of fine and coarse spherical particles above Athens and Bucharest. Due to the exceptional characteristics of the ChArMEx database, the analysis of the microphysical properties profiles temporal evolution was also possible. An in depth analysis was performed mainly at Granada station because of the availability of continuous lidar measurements and frequent AERONET inversion retrievals. The analysis at Granada was of special interest since the station was affected by mineral dust during the complete analyzed period. LIRIC was found to be a very useful tool for performing continuous monitoring of mineral dust, allowing for the analysis of the dynamics of the dust event in the vertical and temporal coordinates. Results obtained here illustrate the importance of having collocated and simultaneous advanced lidar and sun-photometer measurements in order to characterize the aerosol microphysical properties both in the vertical and temporal coordinates at a regional scale. In addition, this study revealed that the use of the depolarization information as input in LIRIC in the stations of Bucharest, Évora and Granada was crucial for the characterization of the aerosol types and their distribution in the vertical column, whereas in stations lacking of depolarization lidar channels ancillary information was needed. Results obtained were also used for the validation of different mineral dust models. In general, the models better

ACPD
15, 32831–32887, 2015

forecast the vertical distribution of the mineral dust than the column integrated mass concentration, which was underestimated in most of the cases.

1 Introduction

The influence of the atmospheric aerosol particles in the Earth's radiative forcing is still affected by a large uncertainty, as indicated in the AR5 report from the Intergovernmental Panel for Climate Change (IPCC, 2013). During past years, this uncertainty has been reduced from high to medium with respect to the data in the Fourth Assessment Report (AR4) of the IPCC, (2007). However, atmospheric aerosol still contribute to the largest uncertainty to the total radiative forcing estimate, even though the level of confidence on the effects of atmospheric aerosols has increased from low and medium to medium and high (for indirect and direct effect, respectively) (IPCC, 2013).

The difficulty in accurately determining atmospheric aerosol properties and their influence on the Earth's radiative forcing lies in their large spatial and temporal variability. Ground based (active and passive) remote sensing techniques have proven to be quite robust and provide accurate results for atmospheric aerosol characterization (e. g. Nakajima et al., 1996; Dubovik and King, 2000; Mattis et al., 2004; Olmo et al., 2006). Nonetheless, they provide information about atmospheric aerosol properties on a local scale. Since regional analyses are highly important when analyzing the aerosol variability, several observational networks have been developed. Namely, the lidar network GALION (Global Atmospheric Watch Aerosol Lidar Observation Network), which includes EARLINET (European Aerosol Research Lidar Network, www.earlinet.org) (Bösenberg et al., 2001; Pappalardo et al., 2014), MPLNET (Micro Pulse Lidar Network) (Welton et al., 2005), LALINET (Latin American Lidar Network, www.lalinet.org) (Guerrero-Rascado et al., 2014) and ADNET (Asian Dust Network) (Shimizu et al., 2004) among others; ant the sun-photometer networks SKYNET (Skyradiometer network) (Takamura and Nakajima, 2004) and AERONET (Aerosol Robotic Network, http://aeronet.gsfc.nasa.gov/) (Holben et al., 1998).

ACPD
15, 32831–32887, 2015

In addition to the regional coverage, these networks can provide useful information on the vertical and temporal coordinates, if adequate measurement protocols are stablished. Information on the vertical structure of the aerosol is of high importance, since the atmospheric aerosol effects can be very different near the surface, within the boundary layer, and in the free troposphere. Estimates of radiative forcing are sensitive to the vertical distribution of aerosols (Claquin et al., 1998; Huang et al., 2009; Sicard et al., 2014) and the vertical information is required for accounting the indirect effect (McCormick et al., 1993; Bréon, 2006). In addition, atmospheric aerosol can change the vertical profile of temperature and atmospheric stability, which in turn influences the wind speed profile within the lower atmosphere (Pérez et al., 2006; Guerrero-Rascado et al., 2009; Choobari et al., 2014). Furthermore, continuous and/or regular measurements provided by the networks, would allow us to analyse the temporal evolution and dynamics of the atmospheric aerosol particles, which will be very useful not only for accurately determining the radiative forcing, but also to improve the performance of numerical weather prediction (NWP) (e.g. Pérez et al., 2006a) and climatological models (Nabat et al., 2014, 2015).

Lidar systems are widely used to determine the vertical distribution of aerosols. There are already many regional studies on the vertical characterization of optical properties based on lidar systems (e. g. Papayannis et al., 2008). However, the characterization of the microphysical properties profiles is still not so straightforward, due to the complexity of the retrievals. Algorithms designed to combine lidar and sun-photometer measurements have been developed in order to overcome this difficulty (e.g. LIdar Radiometer Inversion Code, LIRIC, Chaikovsky et al., 2008, 2012) and Generalized Aerosol Retrieval from Radiometer and Lidar Combined data, GARRLIC (Lopatin et al., 2013). The combination of simultaneous information about the aerosol vertical structure provided by the lidar system and the columnar properties provided by the sun photometer has proven to be a promising synergetic tool for this purpose. LIRIC, which is used in this study, has already provided interesting results about vertically resolved aerosol microphysical properties for selected case studies (Tsekeri et al., 2013; Wag-

ACPD
15, 32831–32887, 2015

ner et al., 2013; Granados-Muñoz et al., 2014, 2015; Papayannis et al., 2014; Binietoglou et al., 2015). The increasing number of stations performing these simultaneous measurements foresees an optimistic future concerning the increasing spatial coverage.

Regional studies in the Mediterranean region are of huge scientific interest since multiple studies indicate that aerosol radiative forcing over the Mediterranean region is one of the largest in the world (Lelieveld et al., 2002; IPCC, 2013). In this context, the ChArMEx (the Chemistry-Aerosol Mediterranean Experiment, http://charmex.lsce.ipsl.fr/) (Dulac et al., 2014) international project involving several Mediterranean countries aims at developing and coordinating regional research actions for a scientific assessment of the present and future state of the atmospheric environment in the Mediterranean Basin, and of its impacts on the regional climate, air quality, and marine biogeochemistry. The ChArMEx project organized a field campaign between 25 June and 12 July 2012, in order to address interactions such as long range transport and air quality, and aerosol vertical structure and sources. The period of the campaign falls within the ACTRIS (Aerosols, Clouds, and Trace Gases Research Infrastructure Network) summer 2012 campaign (8 June–17 July 2012) that aimed at giving support to both ChArMEx and EMEP (European Monitoring and Evaluation Programme) (Espen Yttri et al., 2012) field campaigns. Within the ACTRIS summer 2012 campaign, the European lidar network (EARLINET) (Pappalardo et al., 2014) performed a controlled exercise of feasibility to demonstrate its potential to perform operational, coordinated measurements (Sicard et al., 2015). The exercise consisted of continuous lidar measurements during a 72 h period in July 2012 at different European sites. Most of those lidar data have been successfully assimilated by a regional particulate air quality model to improve 36 h operational aerosol forecasts both in terms of surface PM and aerosol optical depth (Wang et al., 2014).

Our study takes advantage of those continuous lidar measurements combined with simultaneous sun-photometer data to perform a characterization of the vertical distribution of the aerosol microphysical properties at different European stations with LIRIC.

ACPD
15, 32831–32887, 2015

Temporal evolution of the aerosol microphysical properties is also analysed when the continuity of the inverted data is available. Up to our knowledge, it is the first time that LIRIC algorithm is applied in a continuous and automated way to retrieve simultaneous and continuous data acquired at different stations, proving the algorithm capability to provide reliable microphysical properties information with high spatial and temporal resolution. In addition, this exceptional aerosol observational database is used for the spatio-temporal evaluation of different regional mineral dust models

2 Measurement strategy

During the summer of 2012, an intensive measurement campaign was performed in the framework of ChArMEx and EMEP in the Mediterranean Basin at twelve ground-based lidar stations throughout Europe. The main aim of these measurements was to obtain an experimental vertically-resolved database for investigating aerosol radiative impacts over the Mediterranean basin using 3-D regional climate models. The extensive lidar database acquired during this campaign combined with AERONET regular measurements represents a unique opportunity to evaluate the performance of LIRIC microphysical inversion retrieval during the event in both temporal and spatial (horizontal and vertical) coordinates, proving the utility of combined measurements and the potential of LIRIC algorithm for routinary aerosol microphysical properties measurements.

The measurement campaign consisted in 72 h of continuous and simultaneous lidar measurements performed at twelve European stations, with eleven out of them participating in ACTRIS/EARLINET (Sicard et al., 2015). The measurement period started on 9 July at 06:00 UTC and lasted until 12 July 2012 at 06:00 UTC, in coincidence with a forecast mineral dust event over the Mediterranean basin according to dust transport models.

LIRIC algorithm requires lidar data at least in 3 different wavelengths and simultaneous AERONET retrievals in order to obtain the aerosol microphysical properties

ACPD
15, 32831–32887, 2015

profiles. Therefore, to evaluate the performance of LIRIC algorithm and characterize the distribution and temporal evolution of the aerosol microphysical properties during the event, only those stations where multiwavelenght lidar data at 3 wavelengths and AERONET data were available for the period 9–11 July were selected. Namely, those stations were Athens (AT), Barcelona (BA), Bucharest (BU), Évora (EV) and Granada (GR) (Fig. 1). The main characteristics of each station are included in Table 1.

All the five stations are part of both EARLINET and AERONET networks. Thus, these five stations are equipped with at least a multiwavelength lidar and a sun photometer. Multiwavelength lidar systems are used in this study to measure vertical profiles of the atmospheric aerosol properties. Lidar systems in all these five stations emit and receive at least at three different wavelengths (355, 532 and 1064 nm), with the systems in Granada, Bucharest and Évora including depolarization capabilities at 532 nm (Table 1). Depolarization information can be used in the retrieval of the aerosol microphysical properties profiles with LIRIC to distinguish between coarse spherical and coarse spheroid mode.

Stations are also equipped with collocated standard sun photometers CIMEL CE-318-4, used in the AERONET network. AERONET retrieval algorithm provides atmospheric aerosol properties integrated in the atmospheric vertical column (Dubovik and King, 2000; Dubovik et al., 2006). The automatic tracking sun and sky scanning radiometer makes sun direct measurements with a 1.2° full field of view every 15 min at different nominal wavelengths, depending on the station (Table 1). These solar extinction measurements are used to compute aerosol optical depth (τ_λ) at each wavelength except for the 940 nm channel, which is used to retrieve total column water vapour (or precipitable water) (Estellés et al., 2006; Pérez-Ramírez et al., 2012). The estimated uncertainty in computed τ_λ, due primarily to calibration uncertainty, is around 0.01–0.02 for field instruments (which is spectrally dependent, with the larger errors in the UV) (Eck et al., 1999; Estellés et al., 2006).

ACPD
15, 32831–32887, 2015

3 Methodology

3.1 Retrieval of aerosol properties from remote sensing measurements

The analysis of aerosol microphysical properties profiles is performed with LIRIC algorithm. Details about LIRIC retrieval algorithm and its physical basics can be found in previous studies (Chaikovsky et al., 2012, 2015; Kokkalis et al., 2013; Wagner et al., 2013; Granados-Muñoz et al., 2014, 2015; Perrone et al., 2014; Binietoglou et al., 2015), but a brief description is included here for completeness. LIRIC provides profiles of atmospheric aerosol microphysical properties from atmospheric aerosol columnar optical and microphysical properties retrieved from direct sun and sky radiance measurements from the sun-photometer using AERONET code (Version 2, Level 1.5) (Dubovik and King, 2000; Dubovik et al., 2006) and measured lidar elastic backscatter signals at three different wavelengths (355, 532 and 1064 nm). If available, also the 532nm cross-polarized signal is used. Raw lidar data used for this analysis have been prepared accordingly to the EARLINET Single Calculus Chain (SCC), described in detail in D'Amico et al. (2015). From the combination of all this data, volume concentration profiles $C_v(z_n)$ are obtained for fine and coarse aerosol particles. The use of the 532-nm cross-polarized lidar channel allows for distinguishing between spherical and non-spherical particles within the coarse fraction of the aerosol. The uncertainty in LIRIC retrievals associated to the input data is not yet well described, but the algorithm has proven to be very stable and the variations in the output profiles associated to the user-defined input parameters are below 20 % (Granados-Muñoz et al., 2014).

3.2 Model description and validation strategy

Models of dust emission, transport and deposition are used as a tool to understand the various aspects that control the distribution and impact of dust. While global models of the dust cycle are used to investigate dust at large scales and long-term changes, regional dust models are the ideal tool to study in detail the processes that influence dust

ACPD
15, 32831–32887, 2015

distribution as well as individual dust events. The analysis of the aerosol microphysical properties with LIRIC using ChArMEx comprehensive database was used here for the evaluation of a set of 4 regional mineral dust models. This model evaluation was performed for both the vertical and horizontal coordinates and the temporal evolution.

Firstly, the spatial distribution of the mineral dust was examined by using the experimental data from the five EARLINET/AERONET sites considered in the present study. Dust optical depth (at 550 nm) provided by four different regional mineral dust models (BSC-DREAM8b, NMMB/BSC-Dust, DREAM8-NMME and the regional version of COSMO-MUSCAT) was used at this stage. Experimental data were used here just to corroborate the presence or non-presence of mineral dust at the different regions and periods indicated by the models.

BSC-DREAM8b and DREAM8-NMME models are based on the Dust Regional Atmospheric Model (DREAM), originally developed by Nickovic et al. (2001). The main feature of the updated version of the model, BSC-DREAM8b (version 2), include an 8-bins size distribution within the 0.1–10 µm radius range according to Tegen and Lacis (1996), radiative feedbacks (Pérez et al., 2006a, b) and upgrades in its source mask (Basart et al., 2012). BSC-DREAM8b model provides daily dust forecasts at Barcelona Supercomputing Center-Centro Nacional de Supercomputación (BSC-CNS, http://www.bsc.es/projects/earthscience/BSC-DREAM/). The model has been extensively evaluated against observations (see, e.g. Basart et al., 2012b). DREAM8-NMME model (Vukovic et al., 2014), driven by the NCEP Nonhydrostatic Mesoscale Model on E-grid (Janjic et al., 2001), provides daily dust forecasts available at the South East European Virtual Climate Change Center (SEEVCCC; http://www.seevccc.rs/).

NMMB/BSC-Dust model (Pérez et al., 2011; Haustein et al., 2012) is a regional to global dust forecast operational system developed and maintained at BSC-CNS. It is an online multi-scale atmospheric dust model designed and developed at BSC-CNS in collaboration with NOAA-NCEP, NASA Goddard Institute for Space Studies and the International Research Institute for Climate and Society (IRI). NMMB/BSC-Dust model includes a physically based dust emission scheme, which explicitly takes into account

ACPD
15, 32831–32887, 2015

saltation and sandblasting processes. It includes an 8-bin size distribution and radiative interactions. NMMB/BSC-Dust model has been evaluated at regional and global scales (Pérez et al., 2011; Haustein et al., 2012; Gama et al., 2015).

BSC-DREAM8b, NMMB/BSC-DDUST and DREAM8-NMME models are participating in the World Meteorological Organization Sand and Dust Storm Warning Advisory and Assessment System (WMO SDS-WAS) Northern Africa-Middle East-Europe (NAMEE) Regional Center (http://sds-was.aemet.es//). Additionally, NMMB/BSC-Dust is the model that provides operational dust forecast in the first Regional Specialized Meteorological Center with activity specialization on Atmospheric Sand and Dust Forecast, the Barcelona Dust Forecast Center (BDFC; http://dust.aemet.es/).

On the other hand, COSMO-MUSCAT is an online coupled model system based on a different philosophy: COSMO is a non-hydrostatic and compressible meteorological model which solves the governing equations on the basis of a terrain-following grid (Schättler et al., 2008; Baldauf et al., 2011), whereas MUSCAT is a chemistry transport model that treats the atmospheric transport as well as chemical transformations for several gas phase species and particle populations using COSMO output data (Knoth and Wolke, 1998; Wolke et al., 2012). More details about COSMO-MUSCAT model can be found elsewhere (Schepanski et al., 2007, 2009; Heinold et al., 2009; Laurent et al., 2010; Tegen et al., 2013).

The spatial resolution, domain size, initial and boundary conditions, differ, in addition to the different physical parameterizations implemented in the models. Details on the individual mineral dust models and their respective model configurations evaluated here are summarized in Table 2.

Modelled mineral dust mass concentration profiles provided by the previous models were compared with LIRIC output profiles in order to evaluate the model performance on the vertical coordinate. The temporal evolution of the modelled vertical profiles was evaluated in more detail only at Granada, which was the station most affected by the dust outbreak during the analysed period and thus provided a more extensive database. Since LIRIC provides volume concentration profiles, a conversion factor was

ACPD
15, 32831–32887, 2015

needed to obtain mass concentration. This conversion factor was the density of the aerosol particles, namely 2.65 g cm^{-3} for the coarse mode (1–10 µm) and 2.5 g cm^{-3} (0.1–1 µm) for the fine mode (Pérez et al., 2006a, b). In addition, the initial vertical resolution of the different models and LIRIC was established to a common value of 100 m, in order to obtain a compromise between the loss of information from LIRIC and from the different models, following a similar procedure to that in Binietoglou et al. (2015).

After this processing, mineral dust mass concentration profiles provided by BSC-DREAM8b, NMMB/BSC-DUST, DREAM8-NMME and COSMO-MUSCAT models were evaluated against LIRIC results in those cases when mineral dust was detected. For the comparison, the fine mode was assumed to be fine mineral dust since it is not possible to distinguish which part of the fine mode corresponds to dust or non-dust particles with LIRIC. This assumption may cause an overestimation of the mineral dust concentration that becomes more important in those cases with high concentrations of the fine mode (which was not the case in our study). Alternative methods, such as POLIPHON (Polarization-lidar photometer networking) method, could be applied to overcome this difficulty (Mamouri and Ansmann, 2014), but this is out of the scope of our study.

In our study, model output profiles were retrieved every 3 h and compared to LIRIC retrievals during the three analyzed days. Only daytime data are presented here (from 06:00 to18:00 UTC) because of the limitations of LIRIC retrieval during night-time. Due to the difficulties of the models to correctly represent the convective processes occurring within the planetary boundary layer and PBL-free troposphere interactions and the photochemical reactions producing secondary aerosols at the considered resolution, the lowermost part of LIRIC profiles (affected by these processes) was not considered in the comparison presented here. Only data between 2000 m a.s.l., which is the mean value of the PBL height during summer at Granada (Granados-Muñoz et al., 2012), and the highest value (up to between 5 and 6 km) provided by LIRIC were included in the comparisons.

ACPD
15, 32831–32887, 2015

In order to quantify the model agreement with the total dust load observed in the profiles, the dust mass concentration from the different profiles was integrated between 2 and 8 km a.s.l. Relative differences were calculated according to Eq. (1), where n is the number of height levels and C_{mass} (z_n) is the dust mass concentration at each height level z_n:

$$\text{RD} = 100 \times \frac{\sum_n \left(C_{\text{mass}}^{\text{model}}(z_n) - C_{\text{mass}}^{\text{LIRIC}}(z_n) / C_{\text{mass}}^{\text{LIRIC}}(z_n) \right)}{n} \quad (1)$$

The altitude of the center of mass of the dust column (C_{m}) is calculated according to Eq. (2), where z_{min} and z_{max} are 2 and 8 km a.s.l. respectively:

$$C_{\text{m}} = 100 \times \frac{\int_{z_{\text{min}}}^{z_{\text{max}}} z_n C_{\text{mass}}(z_n) \text{d}z_n}{\int_{z_{\text{min}}}^{z_{\text{max}}} C_{\text{mass}}(z_n) \text{d}z_n} \quad (2)$$

A detailed comparison of BSC-DREAM8b, NMMB/BSC-DUST, DREAM8-NMME dust mass concentration profiles with LIRIC results was performed in Binietoglou et al. (2015) using additional stations and selected case studies for the period 2011–2013. However, due to the characteristics of ChArMEx database this study goes a step further and a validation of the mass concentration profiles temporal evolution of a specific mineral dust event is presented for the first time.

4 Results

4.1 Spatial–temporal characterization of aerosol microphysical properties during ChArMEx/EMEP 2012

During the 72 h intensive measurement period, information from different models, platforms and instrumentation was available. A detailed characterization of the situation

ACPD
15, 32831–32887, 2015

above the Mediterranean Basin during the campaign regarding aerosol properties using the different resources available is presented in the following subsections. Characterization of the column-integrated properties is presented in the first place, followed by the analysis of the vertical distribution.

4.1.1 Satellite and column-integrated model forecasts

Aerosol optical products from satellite information were used to obtain a general overview of the mineral dust event. Figure 2 shows the standard aerosol optical depth product retrieved using the dark-target approach from MODIS/Terra (Remer et al., 2005 and references therein) and the AERUS-GEO from MSG/SEVIRI (Carrer et al., 2014) for the three analysed days (9–11 July 2012).

Satellite data evidenced the presence of an aerosol plume extending from the North African coast towards the East with higher aerosol load, as τ_λ values from MODIS sensor indicate, mainly affecting the South-East of the Iberian Peninsula and the South of Italy (Fig. 2). A different aerosol plume can be observed above the Balkans area. The pathways of the aerosol plumes suggested by satellite data are in agreement with both the meteorological analyses of ECMWF and HYSPLIT air mass trajectories based on GDAS analysed meteorological fields at 2 km a.g.l. presented in the study by Wang et al. (2014). The air masses were moving from Spain and Portugal to the East whereas in the Balkans region they were moving southwards.

$\tau_{550\,nm}$ data simulated by BSC-DREAM8b, DREAM8-NMME NMMB/BSC-Dust and COSMO-MUSCAT are shown in Fig. 3, where it is observed that a dust event was affecting a large region in the western Mediterranean basin. Granada station was affected by the mineral dust outbreak during the whole analyzed period according to the four models. The stations of Évora and Barcelona were not affected by the dust event according to BSC-DREAM8b, DREAM8-NMME and NMMB/BSC-Dust, even though Barcelona was located close to the edge according to BSC-DREAM8b. COSMO-MUSCAT indicated the presence of low mineral dust load in both Barcelona and Évora during the three days, but values were almost negligible. In the Eastern re-

ACPD
15, 32831–32887, 2015

gion, the station of Athens was affected by the mineral dust during the three days according to DREAM8-NMME model and COSMO-MUSCAT, only on 10 July according to NMMB/BSC-Dust and on 10 and 11 July according to BSC-DREAM8b. BSC-DREAM8b foresaw no influence of the mineral dust over Bucharest, whereas according to DREAM8-NMME the station was at the edge of the mineral dust plume on 10 and 11 July. NNMB/BSC-DUST indicated a slight presence of mineral dust over Bucharest on, 10 July and COSMO-MUSCAT forecast mineral dust during the three days, with larger loads on 10 and 11 July. In general, it can be observed that larger aerosol loads were forecast by DREAM8-NMME and COSMO-MUSCAT models than by BSC-DREAM8b and NMMB/BSC-Dust. Besides, the different models forecast the dust plume leaving the North of Africa and moving towards the East, as also indicated by satellite data. However, the decrease in $\tau_{550\,nm}$ values with time observed with satellite data is not well captured by the different models.

4.1.2 Ground-based measurements

Data provided by the ground-based instrumentation were also used for the study. Figure 4 shows the time series of the $\tau_{440\,nm}$ and AE(440–880 nm) obtained with the AERONET sun photometers for the selected five stations during the analysed period and mean values for each day and station are indicated in Table 3.

According to these data, the lowest values of $\tau_{440\,nm}$ were measured at Évora station during the whole period, with values below 0.18. The AE(440–880 nm) was close to one, except in the early morning and late evening, when it decreased down to ~ 0.5. These values, together with the columnar volume size distributions observed in Fig. 4c indicates a very low aerosol load, mostly related to aerosol from local sources, and no impact of the North African aerosol plume arriving at the Iberian Peninsula. This is in agreement with the information provided satellites and the set of models, except COSMO-MUSCAT.

A decrease of $\tau_{440\,nm}$ value was observed at Granada station, with maximum values reaching up to 0.40 on the 9 July around 16:00 UTC. During 10 and 11 July,

ACPD
15, 32831–32887, 2015

$\tau_{440\,nm}$ values were between 0.10 and 0.20, except for the late afternoon of 10 July from 17:00 UTC, when the aerosol load decreased and $\tau_{440\,nm}$ below 0.10 were observed. On the contrary, values of the AE(440–870 nm) were increasing from 0.3 on 9 July up to 0.7 on 11 July, with maximum values on the late evening on the 10 July (AE(440–870 nm) > 1). It is worthy to note that the AE(440–870 nm) was below 0.5 during the whole period except for the late afternoon on 10 July, in coincidence with the decrease in $\tau_{440\,nm,}$ indicating a clear predominance of coarse particles (e. g. Pérez et al., 2006a; Basart et al., 2009; Valenzuela et al., 2014). The columnar volume size distributions for the different days agreed with these data. Data from the 9 July showed a very large coarse mode and a small contribution of fine particles. The contribution of fine particles is almost constant during the three days, whereas the coarse mode is decreasing with time. There was a predominance of the coarse mode during the whole period, with maximum values of 0.13 $\mu m^3\,\mu m^{-2}$ during the first day. All these data are usually related to the presence of mineral dust in the station and the temporal evolution of the analyzed properties clearly suggest a decrease of the mineral dust event intensity throughout the analysed period and a possible mixing or aging of the mineral dust. Models in Fig. 3 correctly forecast the arrival of mineral dust above the station, even though they underestimated the aerosol load.

At Barcelona station no AERONET data were available on 9 July. During 10 and 11 July, $\tau_{440\,nm}$ values were relatively high and quite constant (around 0.30) and the AE(440–870 nm) values were larger than 1.5, indicating a strong contribution of fine aerosol particles. In the columnar volume size distributions, similar values for the fine and coarse mode were observed on the 10 July, but larger values of the fine mode were obtained on 11 July. Therefore, it can be inferred from these data that the impact of the North African aerosol plume was almost negligible at this station. It is worthy to note that only COSMO-MUSCAT model forecast a slight presence of dust.

In Athens and Bucharest the aerosol plume presented very different characteristics to those observed on the Western region, as already observed in the satellite data (Fig. 3).

ACPD
15, 32831–32887, 2015

In this region, large $\tau_{440\,nm}$ values (> 0.35) and large values of the AE(440–870 nm) suggested a situation with high aerosol load mainly composed of fine particles. At Athens both $\tau_{440\,nm}$ and AE(440–870 nm) values were very constant during the three analysed days, except for a slight decrease of the AE(440–870 nm) on 11 July (from ∼ 1.70 to ∼ 1.30). This is in agreement with the columnar volume size distributions (Fig. 4c), where a slight increase of the coarse mode was observed on 11 July when compared to 9 and 10 July. In the case of Bucharest, $\tau_{440\,nm}$ was almost constant on 9 and 10 July (around 0.37), but increased on 11 July (over 0.60). The AE(440–870 nm) was almost constant around 1.10 during the three days, indicating a balanced presence of coarse and fine particles. The columnar volume size distributions were very similar to those of Athens on 9 and 10 July, but larger presence of fine particles was observed here on 11 July. According to these sun-photometer data, the aerosol plume over this region was not composed of mineral dust particles, even though low concentrations of mineral dust might have been advected over Athens on 11 July. Therefore, COSMO-MUSCAT dust simulations do not match well the measurements over Athens and Bucharest, whereas the BSC-DREAM8b, NNMB/BSC-DUST and DREAM8-NMME models correctly predicted the situation above Bucharest, but not above Athens station.

4.1.3 Aerosol vertical distribution

Figure 5 shows the time series of the lidar range-corrected signal (RCS) in arbitrary units at 532 nm (at 1064 nm in Athens) for the 72 h period at the different stations. From these plots, it is clearly observed that at Barcelona and Évora the aerosol load was mainly confined within the planetary boundary layer and the time series reveal the evolution of the planetary boundary layer height. Therefore, it is expected that most of the aerosol particles were from local origin. However, at the rest of the stations a more complex vertical structure was observed and the presence of lofted aerosol layer reaching up to 6 km a.s.l. at some periods indicated the advection of different aerosol types.

ACPD
15, 32831–32887, 2015

The aerosol microphysical properties profiles retrieved with LIRIC for different periods at the different stations are shown in Fig. 6. Namely, the volume concentration profiles of the total coarse mode and the fine mode were retrieved at Barcelona and Athens, whereas the volume concentration profiles of fine, coarse spherical and coarse spheroid mode were retrieved at Évora, Bucharest and Granada because of the availability of depolarization information.

At Évora it was clearly observed that the aerosol was located below 1000 m a.s.l., within the planetary boundary layer, and concentrations were very low, ranging from 25 to 46 $\mu m\,cm^{-3}$. At Granada a clear predominance of the coarse spheroid mode in concentrations up to 50 $\mu m^3\,cm^{-3}$ and reaching altitudes around 6000 m a.s.l. was observed, related to a strong presence of mineral dust. Concentrations were decreasing with time and a small contribution of fine particles was also observed during the three days. At Barcelona, the coarse mode particles were predominant in the height range between the surface and 1000 m a.s.l. on 10 July and a similar concentration of fine and coarse particles was observed between 1000 and 2500 m a.s.l. However, on 11 July an aerosol layer dominated by fine particles with a slight presence of coarse particles was observed between 2000 and 4000 m a.s.l. The 5 day backward trajectories analysis performed with HYSPLIT model (Draxler and Rolph, 2003) for Barcelona station (not shown) together with the information of the models previously presented indicates that this upper layer might be related to a faint presence of mineral dust. However, this could also be linked to the presence of biomass burning from the Eastern Iberian Peninsula (see Fig. 7). Depolarization information would be crucial here to discriminate the origin of the aerosol particles arriving at this height above Barcelona. At Athens station the aerosol reached up to 5000 m a.s.l. The coarse mode was located below 2000 m a.s.l., whereas a predominance of fine particles was observed at higher altitudes. The top of the aerosol layer was increasing with time from 3800 to almost 5000 m a.s.l. This temporal evolution of the microphysical properties is coherent with the optical properties shown in Sicard et al., (2015) for the same period. It is worthy to point out that on 11 July, coarse particles were detected between 3000 and 4800 m a.s.l. at this sta-

ACPD
15, 32831–32887, 2015

tion, probably related to the arrival of mineral dust indicated by the models at the end of the period. Backward trajectories analysis with HYSPLIT (not shown) also revealed a change in the trajectory of the air masses arriving at 3500 m a.s.l. which would explain the presence of mineral dust on 11 July. At Bucharest, similar volume concentration of fine and coarse particles was observed on 9 and 10 July. The observed coarse particles were spherical according to LIRIC; therefore the presence of mineral dust at this region can be totally neglected. On 11 July a strong increase of the fine mode volume concentration was observed between 2500 and 5000 m a.s.l. suggesting the advection of an aerosol plume dominated by fine particles at this altitude. Again, this is in agreement with the optical properties presented in Sicard et al. (2015), where a larger spectral dependence (related to finer particles) is observed at Bucharest station in the height range between 3 and 4 km a.s.l., and with the predictions of the dust models participating in the study. As suggested in the study by Sicard et al. (2015) this large spectral dependence of the backscatter coefficient could be originated by the presence of fine particles related to the advection of smoke. The combined information provided by backward trajectories analysis and MODIS FIRMS comes to confirm the presence of active fires along the air masses paths arriving at Bucharest on 11 July (Fig. 7).

The use of the depolarization information as input in LIRIC in the stations of Bucharest, Évora and Granada provided additional information. In the cases of Bucharest and Granada, this information turned out to be very useful for the characterization of the aerosol types and their distribution in the vertical coordinates. The differences in the aerosol type were already evidenced in the columnar volume size distributions retrieved by AERONET code (Fig. 4), and here LIRIC confirmed that these two stations presented really different situations. The volume concentration profiles retrieved with LIRIC indicated a predominance of the spheroid mode in Granada and a predominance of spherical particles in Bucharest, highlighting very different aerosol composition in the coarse mode. However, at stations such as Barcelona or Athens where lidar depolarization was not measured, ancillary information, e.g. backward trajectories or sun-photometer-derived optical properties, was needed to discriminate if

ACPD
15, 32831–32887, 2015

the coarse mode was related to non-spherical particles, usually associated to mineral dust, or to spherical particles, usually present in cases of anthropogenic pollution or aged smoke. Therefore, here we have a clear example of the importance and the potential of the depolarization measurements in the vertical characterization of the aerosol particles.

4.2 Temporal evolution of the aerosol microphysical properties profiles

The continuous analysis of the aerosol microphysical properties profiles during the three days provided very valuable information about the dynamics of the aerosol layers. Because of the uninterrupted lidar measurements at Granada from 12:00 UTC on 9 July 2012 to 00:00 UTC on 12 July and the frequent AERONET retrievals due to good weather conditions a more detailed analysis was performed at this station. A total of 60 different LIRIC retrievals were performed based on 60 lidar datasets and 21 AERONET inversion products.The retrieval of microphysical properties was performed using 30 min averaged lidar data (in order to reduce noise on the lidar profiles) and the closest in time AERONET retrieval, considering only those data with time differences lower than three hours.

Besides, Granada station was affected by a mineral dust event during the whole period as already shown in previous sections. This fact is of special interest since the retrieval of the mineral dust microphysical is not so straightforward and they are not so well characterized. Up to our knowledge not many comprehensive studies on dust microphysical properties vertical profiles have been performed (Tsekeri et al., 2013; Wagner et al., 2013; Granados-Muñoz et al., 2014; Noh, 2014) because of the difficulty of the retrievals due to different factors, e. g. the high temporal variation and non-uniform distribution of dust aerosol concentration around the globe (Sokolik and Toon, 1999; Formenti et al., 2011), mineral dust highly irregular shape and the chemical and physical transformations dust suffers during its transport (Sokolik and Toon, 1999; Chen and Penner, 2005; Formenti et al., 2011).

ACPD
15, 32831–32887, 2015

The dust outbreak analysed here started over Granada station on 7 July in 2012 as indicated by sun-photometer data and the model forecast from previous days (not shown). Thus, it was already well developed when the intensive measurement period started. The presence of mineral dust was correctly forecasted by the different models as depicted in Fig. 3. However, they did not correctly capture the intensity and the temporal evolution of the event. The 5 day backward trajectories analysis performed with HYSPLIT model indicated that the air masses arriving at Granada on 9 and 11 July came from Africa passing by the North African coast above 2500 m a.s.l. and from the North Atlantic Ocean through South-western Iberian Peninsula below this altitude (Fig. 8). On 10 July the air masses came from the central part of Sahara desert through the North African coast for heights above 5000 m a.s.l., from the Atlantic Ocean going along the coast of Africa between 2500 and 5000 m a.s.l. and from the North Atlantic Ocean overpassing South-western Iberian Peninsula below 2500 m a.s.l.

Figure 9 shows the time series of the volume concentration profiles retrieved with LIRIC. It is clearly observed that the dust event was decreasing its intensity along the whole study period with the largest aerosol concentrations for the coarse spheroid mode retrieved on 9 July ($\sim 35\,\mu m^3\,cm^{-3}$) and the lowest concentrations on 11 July ($\sim 15\,\mu m^3\,cm^{-3}$), in agreement with AERONET data and model predictions. Maximum values of total volume concentration were around $60\,\mu m^3\,cm^{-3}$ on 9 July. There was a strong predominance of the coarse spheroid mode during the whole period with maximum values on 9 July in the afternoon, reaching values up to $55\,\mu m^3\,cm^{-3}$. Some fine particles were also observed, with larger volume concentrations during the first day ($\sim 10\,\mu m^3\,cm^{-3}$). For this first day of measurements, fine particles reached altitudes around 6000 m a.s.l., whereas on 10 and 11 July larger volume concentration values were confined to the lowermost region from surface up to 3 km a.s.l. The presence of this fine mode in the upper layers might be related to the advection of anthropogenic pollutants coming from Moroccan industrial activity in the North of Africa mixed with the mineral dust as reported in previous studies (Basart et al., 2009; Rodríguez et al., 2011; Valenzuela et al., 2012, 2014; Lyamani et al., 2014). Figure 8b reveals that air

ACPD
15, 32831–32887, 2015

masses overpassed North African industrial areas before reaching Granada. However, it is also well known that mineral dust emissions produce a submicronic size mode (e.g. Gomes et al., 1990; Alfaro and Gomes, 2001). Depolarization lidar observations over the Mediterranean have illustrated that irregularly shaped fine dust particles significantly contribute to aerosol extinction over the boundary layer during dust transport events (Mamouri and Ansmann, 2014). A more detailed analysis with additional data (e.g. chemical components measurements, single scattering albedo profiles) would be needed in order to come to a quantitative attribution of soil dust and anthropogenic particles to the fine mode.

The contribution of the fine mode in the lowermost part may be due mainly to anthropogenic sources of local origin. From 11 July around 12:00 UTC up to the end of the study period, an increase in the coarse spherical mode concentration was observed. This increase of the coarse spherical mode was associated with a decrease of the particle linear depolarization profiles $\delta^{p}_{532\,nm}$ obtained from the lidar data according to Bravo-Aranda et al. (2013) as shown in Fig. 10. On 9 July the values of $\delta^{p}_{532\,nm}$ were around 0.30 in the layer between 3 and 5 km a.s.l. These values are representative of pure Saharan dust (Freudenthaler et al., 2009). However, they decreased down to 0.25 during the following days, indicating either a possible mixing of dust particles with anthropogenic aerosols or aging processes affecting the mineral dust. During 11 July, the decrease in the fine mode in coincidence with the increase in the coarse spherical mode could be associated to the aging of the mineral dust particles and aggregation processes. On 10 July this behaviour was also faintly observed in the late afternoon.

According to $\delta^{p}_{532\,nm}$ profiles the mineral dust layer was clearly located above 2500 m a.s.l. or even at higher altitudes depending on the analysed period (see Fig. 10). Below this altitude, values were lower indicating more contribution of anthropogenic particles. In the case of LIRIC, these vertical structures were not so clearly defined. Values of the fine and coarse mode volume concentration presented very low variations with height when compared to $\delta^{p}_{532\,nm}$ profiles. This vertical homogeneity is related to the assumption of height independency of properties such as the refractive index, size

ACPD
15, 32831–32887, 2015

distribution of the modes or the sphericity, which according to the results presented in previous studies (Wagner et al., 2013; Granados-Muñoz et al., 2014), is an issue that needs to be carefully considered in the analysis of the results retrieved with LIRIC algorithm.

4.3 Evaluation of the mineral dust models mass concentration vertical profiles

Mineral dust mass concentration profiles provided by the BSC-DREAM8b, NMMB/BSC-Dust, DREAM8-NMME and COSMO-MUSCAT models were evaluated against LIRIC results at Granada in order to evaluate their performance regarding vertical distribution and temporal evolution.

In general, the four models tended to underestimate LIRIC values and to locate the aerosol load at higher altitudes compared to remote sensing results (Figs. 11 and 12). If we analyze the different periods, on 9 July, with $\tau_{440\,nm}$ values around 0.3, a good agreement in the layer between 2500–6000 m a.s.l. for the NMMB/BSC-Dust model was observed. On 10 and 11 July, when $\tau_{440\,nm}$ values were decreasing down to 0.1, lower agreement was observed for the four analyzed models. A good performance of DREAM8-NMME was observed at 06:00 UTC of 10 July, with $\tau_{440\,nm} \sim 0.2$, whereas NMMB/BSC-Dust showed an un-realistic increasing maximum at 5000 m a.s.l. at 15:00 and 18:00 UTC. However, this maximum was very similar to the one provided by LIRIC between 06:00 and 12:00 UTC. Therefore, it could be due to a time shift of the model when compared to the LIRIC values. It is worthy to note that BSC-DREAM8b and NMMB/BSC-Dust use NCEP/FNL data as initial conditions, whereas COSMO-MUSCAT and DREAM8b-NMME use ECWMF, being this a possible cause of the delay in the BSC models. Nonetheless, a more exhaustive analysis with a more comprehensive database would be needed to confirm this hypothesis. COSMO-MUSCAT was showing an increase in the mineral dust load during the analyzed period and a maximum between 4 and 5 km for most of the obtained profiles. Compared to LIRIC retrieved dust concentrations, COSMO-MUSCAT simulates a smoother vertical distribution with too low concentrations during the first half of the 72 h-period and too high

ACPD
15, 32831–32887, 2015

concentrations during the afternoon on 11 July 2012. Taking the vertical resolution of the model into account, the simulation matches well with the LIRIC concentration profile on 11 July. BSC-DREAM8b provided larger values on the 9 July than on 10 and 11 July, as observed also in the experimental data, but it underestimated the aerosol load during the three studied days.

Simulated and observed integrated dust mass concentration values are compared in Fig. 12. On both 10 and 11 July during the afternoon, NMMB/BSC-DUST presented lower differences with LIRIC values and it followed a similar trend to the one observed with LIRIC, with higher values during 9 July decreasing during 10 and 11. DREAM8-NMME and BSC-DREAM8b presented much lower values than LIRIC during the whole analysed period, whereas COSMO-MUSCAT underestimated the aerosol load on 9 and 11 July but overestimated it on 11. In the histogram in Fig. 12d, the relative difference between the different models and LIRIC are presented.

More than 70 % of the data for the four models presented a negative difference because of the underestimation of the mass concentration of the profiles (except for COSMO-MUSCAT), as already observed in Fig. 12a. In the case of BSC-DREAM8b, 80 % of the data had a relative difference in the range between −90 and −30 %, whereas for DREAM8-NMME the range was between −98 and −49 %. For NMMB/BSC-Dust, 80 % of the data were between −97 and 20 % (27 % of the data were overestimating LIRIC values). In the case of COSMO-MUSCAT, 50 % of the data overestimated LIRIC values. In spite of this differences in the mass concentration values, if we focus on the vertical structure of the mineral dust layers provided by the different models we can see that the agreement is quite better. In Fig. 12, it is also depicted the determination coefficient, R^2, which was ranging between 0.01 and 0.84. The largest values were obtained with COSMO-MUSCAT during most of the periods, whereas the lowest values were obtained for NMMB/BSC-Dust on 10 and 11 July and for DREAM8-NMME for the 11 July. The correlation obtained in the present analysis is lower than the ones presented in Binietoglou et al. (2015), where most of the data presented correlation values above 0.5. This is related to the fact that in the study by Binietoglou

ACPD
15, 32831–32887, 2015

et al. (2015) selected mineral dust events with higher aerosol load ($\tau_{440} > 0.15$) were presented whereas in this study the continuous evolution of the dust event was analyzed with τ_{440} ranging between 0.07 and 0.40. R^2 was larger than 0.5 only for 17.5 % of the analyzed profiles and the highest correlation was obtained when the aerosol load was higher. Therefore, models seem to show a better performance in cases of higher aerosol load.

The location of the center of mass, C_m, which is also an indicator of the vertical distribution of the dust mass concentration, is similar in the case of LIRIC and the models (Fig. 12). Despite the models were capable to reproduce the temporal evolution of C_m, in general they tended to locate the dust load at higher altitudes, as indicated by the larger values of C_m obtained. During this event, BSC-DREAM8b model presented the lowest differences with LIRIC regarding C_m height. C_m values determined by DREAM8-NMME model were also very similar to the ones provided by LIRIC on 9 and 10 July but much higher values were obtained on the 11 July, when the mineral dust load was much lower. COSMO-MUSCAT presented lower discrepancies on day 9 and the mornings of 10 and 11 July, whilst NMMB/BSC-Dust presented larger values during the whole period. These results are comparable to those in the study by Binietoglou et al. (2015).

Regarding the discrepancies with LIRIC in the vertical coordinate, Fig. 13 shows that for BSC-DREAM8b, NMMB/BSC-DUST and COSMO-MUSCAT the smallest relative differences in the mass concentration, even though the largest variability, were obtained around 3500 and 4500 m a.s.l. In the cases of NMMB/BSC-Dust and COSMO-MUSCAT, large discrepancies were observed in the upper layer, above 5 km a.s.l. BSC-DREAM8b and DREAM8-NMME underestimated LIRIC values in the whole profile, whereas NMMB/BSC-Dust underestimated LIRIC values below 4.5 km and overestimated the values above 4.5 km. COSMO-MUSCAT overestimated most of the values, except for the height range between 2 and 2.8 km, where we can observe a clear underestimation by all models.

ACPD
15, 32831–32887, 2015

Model profiles were also obtained at the stations of Athens, Barcelona, Bucharest and Évora in order to evaluate their performance at stations where there is a slight or no presence of mineral dust. At Athens (Fig. S1 in the Supplement) almost negligible mass concentration values were forecast by the different models, with the exception of DREAM8-NMME. This model indicated the presence of mineral dust in mass concentrations up to 100 $\mu g\,m^{-3}$ reaching 4000 m a.s.l. on 10 July and up to 65 $\mu g\,m^{-3}$ on the 11 July which is not in agreement with LIRIC results. In spite of the disagreement, it is worthy to point out that the dust layer observed at Athens between 3000 and 5000 m a.s.l. on 11 July according to LIRIC data was correctly forecast by the different models. At Barcelona station (Fig. S2 in the Supplement), DREAM8-NMME were not in agreement with the experimental results since it forecasted dust mass concentrations of up to 100 $\mu g\,m^{-3}$ and located below 2000 m a.s.l. At Bucharest (Fig. S3 in the Supplement), large dust concentrations were forecasted between 3000 and 7000 m a.s.l. by BSC-DREAM8b, DREAM8-NMME and NMMB/BSC-Dust on 9 July. On 10 and 11 July the dust load forecasted by the models was much lower, even though it reached up to 50 $\mu g\,m^{-3}$. This is not in agreement with our experimental results since only coarse spherical and fine particles were observed and no mineral dust should be forecasted here. Finally, at Évora station (Figs. S4 in the Supplement), DREAM8-NMME forecasted dust mass concentration lower than 10 $\mu g\,m^{-3}$ below 2000 m a.s.l. COSMO-MUSCAT forecasted similar concentrations above 2000 m a.s.l. These mass concentration values are almost negligible and therefore good agreement can be considered. In general, good results were provided by the different models at the five stations. However, DREAM8-NMME seems to be overestimating the dust mass concentrations at those stations affected by aerosol types different to mineral dust.

The analysis of the causes for the discrepancies between the models and LIRIC is out of the scope of this study. Understanding the differences between the models and the observations would require wider databases with higher temporal and spatial coverage in order to cover the different aspects of the model calculations (e.g. mineral dust sources, horizontal and vertical transport processes), as already pointed out in

ACPD
15, 32831–32887, 2015

Binietoglou et al., (2015). Nonetheless, the comparison presented here provided valuable results since it addresses the points of discrepancy and proves LIRIC potential as a tool for future model evaluations. Information inferred from the results obtained here could be used for the planning of future validation strategies.

5 Conclusions

In this study, the characterization of aerosol microphysical properties at different stations throughout Europe was performed in the framework of the ChArMEx/EMEP 2012 field campaign, in support to which EARLINET lidar stations performed continuous measurements during the 72 h. LIRIC profiles were obtained at five different stations in Europe (i.e. Athens, Barcelona, Bucharest, Évora and Granada) in order to characterize atmospheric aerosol particles both in the vertical and horizontal coordinates and also their temporal evolution during this period. From the analysis of the aerosol properties at the different stations, two different aerosol plumes were clearly observed: one affecting the Western Mediterranean region, loaded with mineral dust, and another one over the Balkans area, mainly composed of fine particles and coarse spherical particles. Granada station was clearly affected by the mineral dust outbreak during these 72 h, whereas mainly aerosol from local origin was affecting Évora and Barcelona. A mixture of fine and coarse spherical particles was observed over Bucharest, likely related to the presence of smoke from European fires, whereas at Athens mainly fine particles were observed, except on 11 July, when some dust was observed at 3.5 km a.s.l. as indicated by the backward trajectories analysis (not shown).

The availability of LIRIC output profiles at these five different stations provided regional coverage and made possible a comparison with the modelled dust fields. The comparison revealed a quite good agreement with the horizontal distribution of the dust plume forecast by BSC-DREAM8b, NMMB/BSC-Dust and DREAM8-NMME models (based on a similar philosophy), but lower agreement for COSMO-MUSCAT over the Balkans region.

ACPD
15, 32831–32887, 2015

A thorough evaluation of the temporal evolution and the aerosol layers dynamics was possible at Granada station, where a total of 60 lidar profiles every 30 min and 21 AERONET inversion retrievals were available. The analysis of the microphysical properties profiles retrieved with LIRIC indicated that the dust event was decreasing its intensity, with larger concentrations on 9 July ($\sim 55\,\mu m^3\,cm^{-3}$) decreasing towards 11 July ($\sim 15\,\mu m^3\,cm^{-3}$), in agreement with AERONET and satellite data. On 9 July there was a strong predominance of the coarse spheroid mode with maximum values in the afternoon while on 11 July it was observed an increase in the concentration of the coarse spheroid mode during the afternoon up to $15\,\mu m^3\,cm^{-3}$. This temporal evolution of the microphysical properties reveals possible aging processes of the mineral dust above the station or even mixing processes with different aerosol types.

From LIRIC volume concentration profiles, dust mass concentration profiles were derived and compared with the four dust regional models included in the analysis (BSC-DREAM8b, NMMB/BSC-Dust, DREAM8-NMME and COSMO-MUSCAT) every 3 h from 06:00 to 18:00 UTC over the 3 days of interest. The four models tended to underestimate the dust mass concentration when compared to LIRIC results, except for COSMO-MUSCAT on 11 July that overestimated it. The underestimation of the dust mass concentration was around 90 % (180 % overestimation with COSMO-MUSCAT on 11 July). The agreement between LIRIC and the models was better when determining the vertical location of the mineral dust load, even though the models tended to locate the mineral dust at higher altitudes than seen by lidar, as indicated by the determination coefficient values and the center of mass location. The determination coefficient between LIRIC and the models reached values of up to 0.84 (with 50 % of the data with determination coefficients larger than 0.45) and the difference in the center of mass location was below 1 km in 65 % of the cases.

A comparison between LIRIC and the models was also performed at the stations of Évora, Barcelona, Athens and Bucharest. In general, good agreement was obtained for BSC-DREAM8b, NMMB/BSC-Dust and COSMO-MUSCAT when no dust is observed. DREAM8-NMME indicated the presence of mineral dust in large concen-

ACPD
15, 32831–32887, 2015

trations in Athens, Barcelona and Évora, opposite to LIRIC results, which indicated and almost negligible or no presence of mineral dust. BSC-DREAM8b, NMMB/BSC-Dust and DREAM8 forecast the presence of mineral dust in the vertical coordinate in Bucharest station, where LIRIC indicated the presence of a different aerosol type (mostly fine particles).

Summing up, LIRIC proved to be a very powerful tool for the analysis of microphysical properties profiles in those stations with lidar/sun photometer measurements available and our study reveals the importance of the combined regular AERONET/EARLINET measurements for the characterization of aerosol microphysical properties in the vertical, horizontal and spatial coordinates with high resolution. In addition, the advantages on the use of depolarization measurements with lidar systems were also emphasized here, since the stations with depolarization capabilities (namely Bucharest, Évora and Granada) provided much more complete information about the microphysical properties profiles. To come to more robust conclusions a more comprehensive database would be needed in the future in order to improve the input of the models and obtain more accurate forecasts. Regular lidar/sun-photometer combined measurements will provide essential information at this respect.

The Supplement related to this article is available online at doi:10.5194/acpd-15-32831-2015-supplement.

Acknowledgements. This work was supported by the Andalusia Regional Government through projects P12-RNM-2409 and P10-RNM-6299, by the Spanish Ministry of Economy and Competitiveness through projects CGL2013-45410-R, CGL2011-13580-E/CLI, CGL2011-16124-E, and CGL2013-46736-R; by the EU through ACTRIS project (EU INFRA-2010-1.1.16-262254); and by the University of Granada through the contract "Plan Propio. Programa 9. Convocatoria 2013". M. J. Granados-Muñoz was funded under grant AP2009-0552 from the Spanish Ministry of Education and Science. S. N. Pereira was funded under fellowship SFRH/BPD/81132/2011 and projects FCOMP-01-0124-FEDER-029212 (PTDC/GEO-MET/4222/2012 from the Por-

ACPD
15, 32831–32887, 2015

tuguese Government). S. Basart and J. M. Baldasano acknowledge the CICYT project (CGL2010-19652 and CGL2013-46736) and Severo Ochoa Programme (SEV-2011-00067) of the Spanish Government. BSC-DREAM8b and NMMB/BSC-Dust simulations were performed on the Mare Nostrum supercomputer hosted by Barcelona Supercomputing Center-Centro Nacional de Supercomputación (BSC-CNS). This paper was realized also as a part of the project III43007 financed by the Ministry of Education and Science of the Republic of Serbia within the framework of integrated and interdisciplinary research for the period 2011–2015. It has also received funding from the European Union's Seventh Framework Programme for research, technological development and demonstration under grant agreement no 289923 - ITaRS. The CIMEL Calibration was performed at the AERONET-EUROPE calibration center, supported by ACTRIS (European Union Seventh Framework Program) (FP7/2007–2013) under grant agreement no. 262254. The authors express gratitude to the NOAA Air Resources Laboratory for the HYSPLIT transport and dispersion model; the ICARE Data and Services Center the MODIS team; and the ChArMEx project of the multidisciplinary research programme MISTRALS (Mediterranean Integrated Studies at Regional And Local Scales; http://www.mistrals-home.org).

References

Alfaro, S. and Gomes, L.: Modeling mineral aerosol production by wind erosion: intensities and aerosol size distribution in source areas, J. Geophys. Res., 106, 18075–18084, doi:10.1029/2000JD900339, 2001.

Andreae, M.: Biomass burning: its history, use, and distribution and its impact on environmental quality and global climate, in: Global Biomass Burning–Atmospheric, Climatic, and Biospheric Implications, edited by: Levine, J. S., MIT Press, Cambridge, MA, 3–21, 1991.

Basart, S., Pérez, C., Cuevas, E., Baldasano, J. M., and Gobbi, G. P.: Aerosol characterization in Northern Africa, Northeastern Atlantic, Mediterranean Basin and Middle East from direct-sun AERONET observations, Atmos. Chem. Phys., 9, 8265–8282, doi:10.5194/acp-9-8265-2009, 2009.

Basart, S., Pérez, C., Nickovic, S., Cuevas, E., and Baldasano, J. M.: Development and evaluation of the BSC-DREAM8B dust regional model over Northern Africa, the Mediterranean and the Middle East, Tellus B, 64, 18539, doi:10.3402/tellusb.v64i0.18539, 2012.

ACPD
15, 32831–32887, 2015

Binietoglou, I., Basart, S., Alados-Arboledas, L., Amiridis, V., Argyrouli, A., Baars, H., Baldasano, J. M., Balis, D., Belegante, L., Bravo-Aranda, J. A., Burlizzi, P., Carrasco, V., Chaikovsky, A., Comerón, A., D'Amico, G., Filioglou, M., Granados-Muñoz, M. J., Guerrero-Rascado, J. L., Ilic, L., Kokkalis, P., Maurizi, A., Mona, L., Monti, F., Muñoz-Porcar, C., Nicolae, D., Papayannis, A., Pappalardo, G., Pejanovic, G., Pereira, S. N., Perrone, M. R., Pietruczuk, A., Posyniak, M., Rocadenbosch, F., Rodríguez-Gómez, A., Sicard, M., Siomos, N., Szkop, A., Terradellas, E., Tsekeri, A., Vukovic, A., Wandinger, U., and Wagner, J.: A methodology for investigating dust model performance using synergistic EARLINET/AERONET dust concentration retrievals, Atmos. Meas. Tech., 8, 3577–3600, doi:10.5194/amt-8-3577-2015, 2015.

Bosenberg, J., Matthias, V., Amodeo, A., Amiridis, V., Ansmann, A., Baldasano, J. M., Balin, I., Balis, D., Bockmann, C., Boselli, A., Carlsson, G., Chaikovsky, A., Chourdakis, G., Comeron, A., De Tomasi, F., Eixmann, R., Freudenthaler, V., Giehl, H., Grigorov, I., Hagard, A., Iarlori, M., Kirsche, A., Kolarov, G., Komguem, L., Kreipl, S., Kumpf, W., Larcheveque, G., Linne, H., Matthey, R., Mattis, I., Mekler, A., Mironova, I., Mitev, V., Mona, L., Muller, D., Music, S., Nickovic, S., Pandolfi, M., Papayannis, A., Pappalardo, G., Pelon, J., Pérez, C., Perrone, M. R., Persson, R., Resendes, D. P., Rizi, V., Rocadenbosch, F., Rodrigues, J. A., Sauvage, L., Schneidenbach, L., Schumacher, R., Shcherbakov, V., Simeonov, V., Sobolewski, P., Spinelli, N., Stachlewska, I., Stoyanov, D., Trickl, T., Tsaknakis, G., Vaughan, G., Wandinger, U., Wang, X., Wiegner, M., Zavrtanik, M., and Zerefos, C.: EARLINET: a European Aerosol Research Lidar Network to Establish an Aerosol Climatology, Max-Planck Institute für Meteorologie, Report No. 348, ISSN 0937 1060, 2003.

Bravo-Aranda, J. A., Navas-Guzmán, F., Guerrero-Rascado, J. L., Pérez-Ramírez, D., Granados-Muñoz, M. J., and Alados-Arboledas, L.: Analysis of lidar depolarization calibration procedure and application to the atmospheric aerosol characterization, Int. J. Remote Sens., 34, 3543–3560, doi:10.1080/01431161.2012.716546, 2013.

Bréon, F.-M.: How do aerosols affect cloudiness and climate?, Science, 313, 623–624, doi:10.1126/science.1131668, 2006.

Buzzi, A., D'Isidoro, M., and Davolio, S.: A case-study of an orographic cyclone south of the Alps during the MAP SOP, Quarterly, J. Roy. Meteor. Soc., 129, 1795–1818, 2003.

Carrer, D., Ceamanos, X., Six, B., and Roujean, J.-L.: AERUS-GEO: a newly available satellite-derived aerosol optical depth product over Europe and Africa, Geophys. Res. Lett., 41, 7731–7738, doi:10.1002/2014GL061707, 2014.

ACPD
15, 32831–32887, 2015

Chaikovsky, A., Dubovik, O., Goloub, P., Balashevich, N., Lopatsin, A., Karol, Y., Denisov, S. and Lapyonok, T.: Software package for the retrieval of aerosol microphysical properties in the vertical column using combined lidar/photometer data (test version), Technical Report, Minsk, Belarus, Institute of Physics, National Academy of Sciences of Belarus, 2008.

Chaikovsky, A., Dubovik, O., Goloub, P., Tanré, D., Pappalardo, G., Wandinger, U., Chaikovskaya, L., Denisov, S., Grudo, Y., Lopatsin, A., Karol, Y., Lapyonok, T., Korol, M., Osipenko, F., Savitski, D., Slesar, A., Apituley, A., Arboledas, L. A., Binietoglou, I., Kokkalis, P., Granados Muñoz, M. J., Papayannis, A., Perrone, M. R., Pietruczuk, A., Pisani, G., Rocadenbosch, F., Sicard, M., De Tomasi, F., Wagner, J., and Wang, X.: Algorithm and software for the retrieval of vertical aerosol properties using combined lidar/radiometerdata: dissemination in EARLINET, 26th International Laser and Radar Conference, Porto Heli, Greece, 2012.

Chaikovsky, A., Dubovik, O., Holben, B., Bril, A., Goloub, P., Tanré, D., Pappalardo, G., Wandinger, U., Chaikovskaya, L., Denisov, S., Grudo, J., Lopatin, A., Karol, Y., Lapyonok, T., Amiridis, V., Ansmann, A., Apituley, A., Alados-Arboledas, L., Binietoglou, I., Boselli, A., D'Amico, G., Freudenthaler, V., Giles, D., Granados-Muñoz, M. J., Kokkalis, P., Nicolae, D., Oshchepkov, S., Papayannis, A., Perrone, M. R., Pietruczuk, A., Rocadenbosch, F., Sicard, M., Slutsker, I., Talianu, C., De Tomasi, F., Tsekeri, A., Wagner, J., and Wang, X.: Lidar-Radiometer Inversion Code (LIRIC) for the retrieval of vertical aerosol properties from combined lidar/radiometer data: development and distribution in EARLINET, Atmos. Meas. Tech. Discuss., in press, 2015.

Chen, Y. and Penner, J. E.: Uncertainty analysis for estimates of the first indirect aerosol effect, Atmos. Chem. Phys., 5, 2935–2948, doi:10.5194/acp-5-2935-2005, 2005.

Claquin, T., Schulz, M., Balkanski, Y., and Boucher, O.: Uncertainties in assessing radiative forcing by mineral dust, Tellus B, 50, 491–505, doi:10.3402/tellusb.v50i5.16233, 1998.

D'Amico, G., Amodeo, A., Baars, H., Binietoglou, I., Freudenthaler, V., Mattis, I., Wandinger, U., and Pappalardo, G.: EARLINET Single Calculus Chain – general presentation methodology and strategy, Atmos. Meas. Tech. Discuss., 8, 4973–5023, doi:10.5194/amtd-8-4973-2015, 2015.

Draxler, R. R. and Rolph, G. D.: HYSPLIT (HYbrid Single-Particle Lagrangian Integrated Trajectory) model access via NOAA ARL READY website, available at: http://www.arl.noaa.gov/ready/hysplit4.html (last access: 26 January 2015), NOAA Air Resources Laboratory, Silver Spring, Md, 2003.

ACPD
15, 32831–32887, 2015

Dubovik, O. and King, M. D.: A flexible inversion algorithm for retrieval of aerosol optical properties from Sun and sky radiance measurements, J. Geophys. Res., 105, 20673–20696, doi:10.1029/2000JD900282, 2000.

Dubovik, O., Sinyuk, A., Lapyonok, T., Holben, B. N., Mishchenko, M., Yang, P., Eck, T. F., Volten, H, Muñoz, O., and Veihelmann, B.: Application of spheroid models to account for aerosol particle nonsphericity in remote sensing of desert dust, J. Geophys. Res., 111, D11208, doi:10.1029/2005JD006619, 2006.

Dulac, F.: An overview of the Chemistry-Aerosol Mediterranean Experiment (ChArMEx), Geophys. Res. Abstr., EGU2014-11441, EGU General Assembly 2014, Vienna, Austria, 2014.

Eck, T. F., Holben, B. N., Reid, J. S., Dubovik, O., Smirnov, A., O'Neill, N. T., Slutsker, I., and Kinne, S.: Wavelength dependence of the optical depth of biomass burning, urban, and desert dust aerosols, J. Geophys. Res., 104, 31333–31349, doi:10.1029/1999JD900923, 1999.

Espen Yttri, K., Aas, W., Tørseth, K., Kristiansen, N. I., Lund Myhre, C., Tsyro, S., Simpson, D:, Bergström, R., Marečková, K., Wankmüller, R., Klimont, Z., Amman, M., Kouvarakis, G. N., Laj, P., Pappalardo, G., and Prévôt, A.: EMEP co-operative programme for monitoring and evaluation of the long-range transmission of air Pollutants in Europe. Transboundary particulate matter in Europe. Status report 2012, available at: http://www.actris.net/Portals/97/documentation/dissemination/other/emep4-2012.pdf (last access: 9 December 2014), 2012.

Estellés, V., Utrillas, M. P., Martínez-Lozano, J. A., Alcántara, A., Alados-Arboledas, L., Olmo, F. J., Lorente, J., de Cabo, X., Cachorro, V., Horvath, H., Labajo, A., Sorribas, M., Díaz, J. P., Díaz, A. M., Silva, A. M., Elías, T., Pujadas, M., Rodrigues, J. A., Cañada, J., and García, Y.: Intercomparison of spectroradiometers and Sun photometers for the determination of the aerosol optical depth during the VELETA-2002 field campaign, J. Geophys. Res., 111, D17207, doi:10.1029/2005JD006047, 2006.

Formenti, P., Schütz, L., Balkanski, Y., Desboeufs, K., Ebert, M., Kandler, K., Petzold, A., Scheuvens, D., Weinbruch, S., and Zhang, D.: Recent progress in understanding physical and chemical properties of African and Asian mineral dust, Atmos. Chem. Phys., 11, 8231–8256, doi:10.5194/acp-11-8231-2011, 2011.

Freudenthaler, V., Esselborn, M., Wiegner, M., Heese, B., Tesche, M., Ansmann, A., Müller, D., Althausen, A., Wirth, M., and Fix, A.: Depolarization ratio profiling at several wavelengths in pure Saharan dust during SAMUM 2006, Tellus B, 61, 165–179, doi:10.1111/j.1600-0889.2008.00396.x, 2009.

ACPD
15, 32831–32887, 2015

Ginoux, P., Chin, M., Tegen, I., Prospero, J. M., Holben, B., Dubovik, O., and Lin, S. J.: Sources and distributions of dust aerosols simulated with the GOCART model, J. Geophys. Res., 106, 20255–20273, doi:0148-0227/01/2000JD000053509.00, 2011.

Gomes, L., Bergametti, G., Coudé-Gaussen, G., and Rognon, P.: Submicron desert dusts: a sandblasting process, J. Geophys. Res., 95, 13927–13935, doi:10.1029/JD095iD09p13927, 1990.

Granados-Muñoz, M. J., Navas-Guzmán, F., Bravo-Aranda, J. A., Guerrero-Rascado, J. L., Lyamani, H., Fernández-Gálvez, J., and Alados-Arboledas, L.: Automatic determination of the planetary boundary layer height using lidar: one-year analysis over southeastern Spain, J. Geophys. Res., 117, D18208, doi:10.1029/2012JD017524, 2012.

Granados-Muñoz, M. J., Guerrero-Rascado, J. L., Bravo-Aranda, J. A., Navas-Guzmán, F., Valenzuela, A., Lyamani, H., Chaikovsky, A., Wandinger, U., Ansmann, A., Dubovik, O., Grudo, J. O., and Alados-Arboledas, L.: Retrieving aerosol microphysical properties by Lidar-Radiometer Inversion Code (LIRIC) for different aerosol types, J. Geophys. Res.-Atmos., 119, 4836–4858 doi:10.1002/2013JD021116, 2014.

Granados-Muñoz, M. J., Bravo-Aranda, J. A., Baumgardner, D., Guerrero-Rascado, J. L., Pérez-Ramírez, D., Navas-Guzmán, F., Veselovskii, I., Lyamani, H., Valenzuela, A., Olmo, F. J., Titos, G., Andrey, J., Chaikovsky, A., Dubovik, O., Gil-Ojeda, M., and Alados-Arboledas, L.: Study of aerosol microphysical properties profiles retrieved from ground-based remote sensing and aircraft in-situ measurements during a Saharan dust event, Atmos. Meas. Tech. Discuss., 8, 9289–9338, doi:10.5194/amtd-8-9289-2015, 2015.

Guerrero-Rascado, J. L., Olmo, F. J., Avilés-Rodríguez, I., Navas-Guzmán, F., Pérez-Ramírez, D., Lyamani, H., and Alados Arboledas, L.: Extreme Saharan dust event over the southern Iberian Peninsula in september 2007: active and passive remote sensing from surface and satellite, Atmos. Chem. Phys., 9, 8453–8469, doi:10.5194/acp-9-8453-2009, 2009.

Guerrero-Rascado, J. L., Landulfo, E., Antuña, J. C., Barbosa, H. M. J., Barja, B., Bastidas, A. E., Bedoya, A. E., da Costa, R., Estevan, R., Forno, R. N., Gouveia, D. A., Jiménez, C., Larroza, E. G., Lopes, F. J. S., Montilla-Rosero, E., Moreira, G. A., Nakaema, W. M., Nisperuza, D., Otero, L., Pallotta, J. V., Papandrea, S., Pawelko, E., Quel, E. J., Ristori, P., Rodrigues, P. F., Salvador, J., Sánchez, M. F., and Silva, A.: Towards an instrumental harmonization in the framework of LALINET: dataset of technical specifications, Proc. SPIE 2014, Vol. 9246, 92460O-1–92460O-14, doi:10.1117/12.2066873, 2014.

ACPD
15, 32831–32887, 2015

Haustein, K., Pérez, C., Baldasano, J. M., Jorba, O., Basart, S., Miller, R. L., Janjic, Z., Black, T., Nickovic, S., Todd, M. C., Washington, R., M uller, D., Tesche, M., Weinzierl, B., Esselborn, M., and Schladitz, A.: Atmospheric dust modeling from meso to global scales with the online NMMB/BSC-Dust model – Part 2: Experimental campaigns in Northern Africa, Atmos. Chem. Phys., 12, 2933–2958, doi:10.5194/acp-12-2933-2012, 2012.

Heinold, B., Tegen, I., Esselborn, M., Kandler, K., Knippertz, P., Müller, D., Schladitz, A., Tesche, M., Weinzierl, B., Ansmann, A., Althausen, D., Laurent, B., Petzold, A., and Schepanski, K.: Regional Saharan dust modelling during the SAMUM 2006 campaign, Tellus B, 61, 307–324, doi:10.1111/j.1600-0889.2008.00387.x, 2009.

Holben, B. N., Eck, T. F., Slutsker, I., Tanré, D., Buis, J. P., Setzer, A., Vermote, E., Reagan, J. A., Kaufman, Y. J., Nakajima, T., Lavenus, F., Jankowiak, I., and Smirnov, A.: AERONET – A federated instrument network and data archive for aerosol characterization, Remote Sens. Environ., 66, 1–16, 1998.

Huang, J., Fu, Q., Su, J., Tang, Q., Minnis, P., Hu, Y., Yi, Y., and Zhao, Q.: Taklimakan dust aerosol radiative heating derived from CALIPSO observations using the Fu-Liou radiation model with CERES constraints, Atmos. Chem. Phys., 9, 4011–4021, doi:10.5194/acp-9-4011-2009, 2009.

IPCC: Contribution of Working Group I to the Fifth Assessment Report of the Intergovernmental Panel on Climate Change Summary for Policymakers in Climate Change, Stocker, Cambrigde University Press, 2013.

Janjic, Z. I., Gerrity Jr., J. P., and Nickovic, S.: An alternative approach to nonhydrostatic modeling, Mon. Weather Rev., 129, 1164–1178, 2001.

Knoth, O. and Wolke, R.: An explicit-implicit numerical approach for atmospheric chemistry-transport modelling, Atmos. Environ., 32, 1785–1797, 1998.

Kokkalis, P., Papayannis, A., Mamouriy, R. E., Tsaknakis, G., and Amiridis, V.: The EOLE lidar system of the National Technical University of Athens, 629–632, 26th International Laser Radar Conference, 25–29 June 2012, Porto Heli, Greece, 2012.

Kokkalis, P., Papayannis, A., Amiridis, V., Mamouri, R. E., Veselovskii, I., Kolgotin, A., Tsaknakis, G., Kristiansen, N. I., Stohl, A., and Mona, L.: Optical, microphysical, mass and geometrical properties of aged volcanic particles observed over Athens, Greece, during the Eyjafjallajökull eruption in April 2010 through synergy of Raman lidar and sunphotometer measurements, Atmos. Chem. Phys., 13, 9303–9320, doi:10.5194/acp-13-9303-2013, 2013.

ACPD
15, 32831–32887, 2015

Kumar, D., Rocadenbosch, F., Sicard, M., Comeron, A., Muñoz, C., Lange, D., Tomás, S., and Gregorio, E.: Six-channel polychromator design and implementation for the UPC elastic/Raman LIDAR, Proc. SPIE, 8182, 81820 W-1-10, 2011.

Laurent, B., Tegen, I., Heinold, B., Schepanski, K., Weinzierl, B., and Esselborn, M.: A model study of Saharan dust emissions and distributions during the SAMUM-1 campaign, J. Geophys. Res., 115, D21210, doi:10.1029/2009JD012995, 2010.

Lopatin, A., Dubovik, O., Chaikovsky, A., Goloub, P., Lapyonok, T., Tanré, D., and Litvinov, P.: Enhancement of aerosol characterization using synergy of lidar and sun-photometer coincident observations: the GARRLiC algorithm, Atmos. Meas. Tech., 6, 2065–2088, doi:10.5194/amt-6-2065-2013, 2013.

Lyamani, H., Valenzuela, A., Perez-Ramirez, D., Toledano, C., Granados-Muñoz, M. J., Olmo, F. J., and Alados-Arboledas, L.: Aerosol properties over the western Mediterranean basin: temporal and spatial variability, Atmos. Chem. Phys., 15, 2473–2486, doi:10.5194/acp-15-2473-2015, 2015.

Mamouri, R. E. and Ansmann, A.: Fine and coarse dust separation with polarization lidar, Atmos. Meas. Tech., 7, 3717–3735, doi:10.5194/amt-7-3717-2014, 2014.

Mattis, I., Ansmann, A., Müller, D., Wandinger, U., and Althausen, D.: Multiyear aerosol observations with dual-wavelength Raman lidar in the framework of EARLINET, J. Geophys. Res., 109, D13203, doi:10.1029/2004JD004600, 2004.

Maurizi, A., D'Isidoro, M., and Mircea, M.: BOLCHEM: an integrated system for atmospheric dynamics and composition, in: Integrated Systems of Meso-Meteorological and Chemical Transport Models, edited by: Baklanov, A., Mahura, A., and Sokhi, R. J., Springer, 89–94, 2011.

McCormick, M. P., Wang, P. H., and Poole, L. R.: Stratospheric aerosols and clouds, in Aerosol-Cloud-Climate Interactions, edited by: Hobbs, P. V., Academic Press, San Diego, California, 205–222, 1993.

Mircea, M., D'Isidoro, M., Maurizi, A., Vitali, L., Monforti, F., Zanini, G., and Tampieri, F.: A comprehensive performance evaluation of the air quality model BOLCHEM to reproduce the ozone concentrations over Italy, Atmos. Environ., 42, 1169–1185, doi:10.1016/j.atmosenv.2007.10.043, 2008.

Nabat, P., Somot, S., Mallet, M., Sanchez-Lorenzo, A., and Wild, M.: Contribution of anthropogenic sulfate aerosols to the changing Euro-Mediterranean climate since 1980, Geophys. Res. Lett., 41, 5605–5611, doi:10.1002/2014GL060798, 2014.

ACPD
15, 32831–32887, 2015

Nabat, P., Somot, S., Mallet, M., Sevault, F., Chiacchio, M., and Wild, M.: Direct and semi-direct aerosol radiative effect on the Mediterranean climate variability using a coupled regional climate system model, Clim. Dynam., 44, 1127–1155, doi:10.1007/s00382-014-2205-6, 2015.

Nakajima, T., Tonna, G., Rao, R., Boi, P., Kaufman, Y., and Holben, B.: Use of sky brightness measurements from ground for remote sensing of particulate polydispersions, Appl. Optics, 35, 2672–2686, doi:10.1364/AO.35.002672, 1996.

Nemuc, A., Vasilescu, J., Talianu, C., Belegante, L., and Nicolae, D.: Assessment of aerosol's mass concentrations from measured linear particle depolarization ratio (vertically resolved) and simulations, Atmos. Meas. Tech., 6, 3243–3255, doi:10.5194/amt-6-3243-2013, 2013.

Nickovic, S., Kallos, K., Papadopoulos, A., and Kakaliagou, O.: A model for prediction of desert dust cycle in the atmosphere, J. Geophys. Res., 106, 18113–18118, doi:10.1029/2000JD900794, 2001.

Noh, Y. M.: Single-scattering albedo profiling of mixed Asian dust plumes with multiwavelength Raman lidar, Atmos. Environ., 95, 305–317, doi:10.1016/j.atmosenv.2014.06.028, 2014.

Olmo, F. J., Quirantes, A., Alcántara, A., Lyamani, H., and Alados-Arboledas, L.: Preliminary results of a non-spherical aerosol method for the retrieval of the atmospheric aerosol optical properties, J. Quant. Spectrosc. Ra., 100, 305–314, doi:10.1016/j.jqsrt.2005.11.047, 2006.

Papayannis, A., Amiridis, V., Mona, L., Tsaknakis, G., Balis, D., Bösenberg, J., Chaikovski, A., De Tomasi, F., Grigorov, I., Mattis, I., Mitev, V., Müller, D., Nickovic, S., Pérez, C., Pietruczuk, A., Pisani, G., Ravetta, F., Rizi, V., Sicard, M., Trickl, T., Wiegner, M., Gerding, M., Mamouri, R. E., D'Amico, G., and Pappalardo, G.: Systematic lidar observations of Saharan dust over Europe in the frame of EARLINET (2000–2002), J. Geophys. Res., 113, D10204, doi:10.1029/2007JD009028, 2008.

Papayannis, A., Nicolae, D., Kokkalis, P., Binietoglou, I., Talianu, C., Belegante, L., Tsaknakis, G., Cazacu, M. M., Vetres, I, and Ilic, L.: Optical, size and mass properties of mixed type aerosols in Greece and Romania as observed by synergy of lidar and sunphotometers in combination with model simulations: a case study, Sci. Total Environ., 500–501, 277–294, doi:10.1016/j.scitotenv.2014.08.101, 2014.

Pappalardo, G., Amodeo, A., Apituley, A., Comeron, A., Freudenthaler, V., Linné, H., Ansmann, A., Bösenberg, J., D'Amico, G., Mattis, I., Mona, L., Wandinger, U., Amiridis, V., Alados-Arboledas, L., Nicolae, D., and Wiegner, M.: EARLINET: towards an advanced sustainable European aerosol lidar network, Atmos. Meas. Tech., 7, 2389–2409, doi:10.5194/amt-7-2389-2014, 2014.

ACPD
15, 32831–32887, 2015

Pérez, C., Nickovic, S., Pejanovic, G., Baldasano, J. M., and Özsoy, E.: Interactive dust-radiation modeling: a step to improve weather forecasts, J. Geophys. Res., 111, D16206, doi:10.1029/2005JD006717, 2006a.

Pérez, C., Nickovic, S., Baldasano, J. M., Sicard, M., Rocadenbosch, F., and Cachorro, V. E.: A long Saharan dust event over the western Mediterranean: lidar, Sun photometer observations, and regional dust modeling? J. Geophys. Res., 111, D15214, doi:10.1029/2005JD006579, 2006b.

Pérez, C., Haustein, K., Janjic, Z., Jorba, O., Huneeus, N., Baldasano, J. M., Black, T., Basart, S., Nickovic, S., Miller, R. L., Perlwitz, J. P., Schulz, M., and Thomson, M.: Atmospheric dust modeling from meso to global scales with the online NMMB/BSC-Dust model – Part 1: Model description, annual simulations and evaluation, Atmos. Chem. Phys., 11, 13001–13027, doi:10.5194/acp-11-13001-2011, 2011.

Pérez-Ramírez, D., Navas-Guzmán, F., Lyamani, H., Fernández-Gálvez, J., Olmo, F. J., Alados-Arboledas, L.: Retrievals of precipitable water vapor using star photometry: assessment with Raman lidar and link to sun photometry, J. Geophys. Res., 117, D05202, doi:10.1029/2011JD016450, 2012.

Perrone, M. R., De Tomasi, F., and Gobbi, G. P.: Vertically resolved aerosol properties by multiwavelength lidar measurements, Atmos. Chem. Phys., 14, 1185–1204, doi:10.5194/acp-14-1185-2014, 2014.

Preißler, J., Wagner, F., Pereira, S. N., and Guerrero-Rascado, J. L.: Multi-instrumental observation of an exceptionally strong Saharan dust outbreak over Portugal, J. Geophys. Res., 116, D24204, doi:10.1029/2011JD016527, 2011.

Remer, L. A., Kaufman, Y. J., Tanré, D., Mattoo, S., Chu, D. A., Martins, J. V., Li, R. R., Ichoku, C., Levy, R. C., Kleidman, R. G., Eck, T. F., Vermote, E., and Holben, B. N.: The MODIS aerosol algorithm, products, and validation, J. Atmos. Sci., 62, 947–973, 2005.

Rodríguez, S., Alastuey, A., Alonso-Pérez, S., Querol, X., Cuevas, E., Abreu-Afonso, J., Viana, M., Pérez, N., Pandolfi, M., and de la Rosa, J.: Transport of desert dust mixed with North African industrial pollutants in the subtropical Saharan Air Layer, Atmos. Chem. Phys., 11, 6663–6685, doi:10.5194/acp-11-6663-2011, 2011.

Schättler, U., Doms, G., and Schraff, C.: A Description of the Nonhydrostatic Regional COSMO-Model, Deutscher Wetterdienst, Offenbach, available at: http://www.cosmo-model.org (last access: 2 November 2015), 2008.

ACPD
15, 32831–32887, 2015

Schepanski, K., Tegen, I., Laurent, B., Heinold, B., and Macke, A.: A new Saharan dust source activation frequency map derived from MSG-SEVIRI IR-channels, Geophys. Res. Lett., 34, L18803, doi:10.1029/2007GL030168, 2007.

Schepanski, K., Tegen, I., and Macke, A.: Saharan dust transport and deposition towards the tropical northern Atlantic, Atmos. Chem. Phys., 9, 1173–1189, doi:10.5194/acp-9-1173-2009, 2009.

Shimizu, A., Sugimoto, N., Matsui, I., Arao, K., Uno, I., Murayama, T., Kagawa, N., Aoki, K., Uchiyama, A., and Yamazaki, A.: Continuous observations of Asian dust and other aerosols by polarization lidars in China and Japan during ACE-Asia, J. Geophys. Res., 109, D19S17, doi:10.1029/2002JD003253, 2004.

Sicard, M., D'Amico, G., Comerón, A., Mona, L., Alados-Arboledas, L., Amodeo, A., Baars, H., Baldasano, J. M., Belegante, L., Binietoglou, I., Bravo-Aranda, J. A., Fernández, A. J., Fréville, P., García-Vizcaíno, D., Giunta, A., Granados-Muñoz, M. J., Guerrero-Rascado, J. L., Hadjimitsis, D., Haefele, A., Hervo, M., Iarlori, M., Kokkalis, P., Lange, D., Mamouri, R. E., Mattis, I., Molero, F., Montoux, N., Muñoz, A., Muñoz Porcar, C., Navas-Guzmán, F., Nicolae, D., Nisantzi, A., Papagiannopoulos, N., Papayannis, A., Pereira, S., Preißler, J., Pujadas, M., Rizi, V., Rocadenbosch, F., Sellegri, K., Simeonov, V., Tsaknakis, G., Wagner, F., and Pappalardo, G.: EARLINET: potential operationality of a research network, Atmos. Meas. Tech., 8, 4587–4613, doi:10.5194/amt-8-4587-2015, 2015.

Sokolik, I. N. and Toon, O. B.: Incorporation of mineralogical composition into models of the radiative properties of mineral aerosol from UV to IR wavelengths, J. Geophys. Res., 104, 9423–9444, 1999.

Spyrou, C., Mitsakou, C., Kallos, G., Louka, P., and Vlastou, G.: An improved limited area model for describing the dust cycle in the atmosphere, J. Geophys. Res., 115, D17211, doi:10.1029/2009JD013682, 2010.

Takamura, T. and Nakajima, T.: Overview of SKYNET and its activities, Opt. Pura Appl, 37, 3303–3308, 2004.

Tegen, I., Schepanski, K., and Heinold, B.: Comparing two years of Saharan dust source activation obtained by regional modelling and satellite observations, Atmos. Chem. Phys., 13, 2381–2390, doi:10.5194/acp-13-2381-2013, 2013.

Textor, C., Schulz, M., Guibert, S., Kinne, S., Balkanski, Y., Bauer, S., Berntsen, T., Berglen, T., Boucher, O., Chin, M., Dentener, F., Diehl, T., Feichter, J., Fillmore, D., Ginoux, P., Gong, S., Grini, A., Hendricks, J., Horowitz, L., Huang, P., Isaksen, I. S. A., Iversen, T., Kloster, S.,

ACPD
15, 32831–32887, 2015

Koch, D., Kirkevåg, A., Kristjansson, J. E., Krol, M., Lauer, A., Lamarque, J. F., Liu, X., Montanaro, V., Myhre, G., Penner, J. E., Pitari, G., Reddy, M. S., Seland, Ø., Stier, P., Takemura, T., and Tie, X.: The effect of harmonized emissions on aerosol properties in global models – an AeroCom experiment, Atmos. Chem. Phys., 7, 4489–4501, doi:10.5194/acp-7-4489-2007, 2007.

Tsekeri, A., Amiridis, V., Kokkalis, P., Basart, S., Chaikovsky, A., Dubovik, O., Papayannis, A., Baldasano, J. M., and Gross, B.: Application of a synergetic lidar and sunphotometer algorithm for the characterization of a dust event over Athens, Greece, British, J. Environ. Clim. Change, 3, 531–546, doi:10.9734/BJECC/2013/2615#sthash.YeD42fFe.dpuf, 2013.

Valenzuela, A., Olmo, F. J., Lyamani, H., Antón, M., Quirantes, A., and Alados-Arboledas, L.: Classification of aerosol radiative properties during African desert dust intrusions over southeastern Spain by sector origins and cluster analysis, J. Geophys. Res., 117, D06214, doi:10.1029/2011JD016885, 2012.

Valenzuela, A., Olmo, F. J., Lyamani, H., Granados-Muñoz, M. J., Antón, M., Guerrero-Rascado, J. L., Quirantes, A., Toledano, C., Perez-Ramírez, D., and Alados-Arboledas, L.: Aerosol transport over the western Mediterranean basin: evidence of the contribution of fine particles to desert dust plumes over Alborán Island, J. Geophys. Res., 119, 14028–14044, doi:10.1002/2014JD022044, 2014.

Vukovic, A., Vujadinovic, M., Pejanovic, G., Andric, J., Kumjian, M. R., Djurdjevic, V., Dacic, M., Prasad, A. K., El-Askary, H. M., Paris, B. C., Petkovic, S., Nickovic, S., and Sprigg, W. A.: Numerical simulation of "an American haboob", Atmos. Chem. Phys., 14, 3211-3230, doi:10.5194/acp-14-3211-2014, 2014.

Wagner, J., Ansmann, A., Wandinger, U., Seifert, P., Schwarz, A., Tesche, M., Chaikovsky, A., and Dubovik, O.: Evaluation of the Lidar/Radiometer Inversion Code (LIRIC) to determine microphysical properties of volcanic and desert dust, Atmos. Meas. Tech., 6, 1707–1724, doi:10.5194/amt-6-1707-2013, 2013.

Wang, Y., Sartelet, K. N., Bocquet, M., Chazette, P., Sicard, M., D'Amico, G., Léon, J. F., Alados-Arboledas, L., Amodeo, A., Augustin, P., Bach, J., Belegante, L., Binietoglou, I., Bush, X., Comerón, A., Delbarre, H., García-Vízcaino, D., Guerrero-Rascado, J. L., Hervo, M., Iarlori, M., Kokkalis, P., Lange, D., Molero, F., Montoux, Muñoz, A., Muñoz, C., Nicolae, D., Papayannis, A., Pappalardo, G., Preissler, J., Rizi, V., Rocadenbosch, F., Sellegri, K., Wagner, F., and Dulac, F.: Assimilation of lidar signals: application to aerosol forecasting in the

ACPD
15, 32831–32887, 2015

western Mediterranean basin, Atmos. Chem. Phys., 14, 12031–12053, doi:10.5194/acp-14-12031-2014, 2014.

Welton, E. J., Campbell, J. R., Berkoff, T. A., Valencia, S., Spinhirne, J. D., Holben, B., and Tsay, S. C.: 5.2 The Nasa Micro-Pulse Lidar Network (MPLNET): co-location of lidars with AERONET sunphotometers and related Earth Science applications, Proc. 85th Annu. Meet. Am. Meteor. Soc., San Diego, 9–13 January 2005, 5165–5169, 2005.

Wolke, R., Schroeder, W., Schroedner, R., and Renner, E.: Influence of grid resolution and meteorological forcing on simulated European air quality: a sensitivity study with the modeling system COSMO-MUSCAT, Atmos. Environ., 53, 110–130, doi:10.1016/j.atmosenv.2012.02.085, 2012.

Zender, C. S., Miller, R., and Tegen, I.: Quantifying mineral dust mass budgets: terminology, constraints, and current estimates, Eos T. Am. Geophys. Un., 85, 509–512, doi:10.1029/2004EO480002, 2004.

ACPD
15, 32831–32887, 2015

Table 1. Lidar and sun-photometer characteristics for the five stations considered in this study and depicted in Fig. 1. A more detailed description of the experimental sites and the lidar systems in every station can be found in the references included in Reference column of the table.

			Lidar characteristics			Sun-photometer characteristics	Reference
Site	Latitude, Longitude	Altitude (m a.s.l.)	Elastic channels (nm)	Raman channels (nm)	System name	Channels (nm)	
AT (Athens)	37.97° N, 23.77° E	200	355, 532, 1064	387, 407, 607	EOLE	340, 380, 440, 500, 675, 870, 1020, 1640	Kokkalis et al. (2012)
BA (Barcelona)	41.39° N, 2.17° E	115	355, 532, 1064	387, 407, 607	UPCLidar	440, 675, 870, 1020	Kumar et al. (2011)
BU (Bucharest)	44.35° N, 26.03° E	93	355, 532 parallel, 532 cross, 1064	387, 407, 607	RALI (LR313-D400)	340, 380, 440, 500, 675, 870, 1020	Nemuc et al. (2013)
EV (Évora)	38.57° N, 7.91° W	293	355, 532, 532 cross, 1064	387, 407, 607	PAOLI	340, 380, 440, 500, 675, 870, 1020, 1640	Preißler et al. (2011)
GR (Granada)	37.16° N, 3.61° W	680	355, 532 parallel, 532 cross, 1064	387, 407, 607	MULHACEN (LR321-D400)	340, 380, 440, 500, 675, 870, 1020	Guerrero-Rascado et al. (2009)

ACPD
15, 32831–32887, 2015

Table 2. Summary of the main parameters of the mineral dust transport models used in this study.

	BSC-DREAM8b	NMMB/BSC-Dust	COSMO-MUSCAT	DREAM8-NMME
Institution	BSC-CNS	BSC-CNS	TROPOS	SEEVCCC/IPB
Meteorological driver	Eta/NCEP	NMMB/NCEP	COSMO	NMME/NCEP
Initial and boundary conditions	NCEP/FNL	NCEP/FNL	GME	ECMWF analysis data in 6 h intervals
Domain	30° W to 65° E and 0 to 65° N	30° W to 65° E and 0 to 65° N	30° W to 35° E and 0 to 60° N	221 × 251 points, 26° W, 62° E, 7° N, 57° N
Resolution	0.33° × 0.33°	0.33° × 0.33°	0.25° × 0.25°	0.2° × 0.2°
Vertical resolution	24 Eta-layers	40 σ-hybrid layers	41 σ-hybrid layers	28 σ-hybrid pressure levels
Radiation interaction	Yes	No activated	Yes, online	No
Data assimilation	No	No	No	No

ACPD
15, 32831–32887, 2015

Table 3. $\tau_{440\,nm}$ and AE(440–870 nm) daily mean values (±standard deviation) at the five stations on 9, 10 and 11 July 2012.

Site	9 Jul $\tau_{440\,nm}$	AE(440–870 nm)	10 Jul $\tau_{440\,nm}$	AE(440–870 nm)	11 Jul $\tau_{440\,nm}$	AE(440–870 nm)
AT	0.51 ± 0.02	1.76 ± 0.01	0.45 ± 0.05	1.67 ± 0.03	0.44 ± 0.01	1.28 ± 0.02
BA	n/d	n/d	0.28 ± 0.01	1.65 ± 0.05	0.27 ± 0.03	1.47 ± 0.01
BU	0.40 ± 0.04	1.08 ± 0.04	0.34 ± 0.04	1.07 ± 0.06	0.62 ± 0.05	1.10 ± 0.05
EV	0.08 ± 0.02	0.82 ± 0.12	0.08 ± 0.01	0.87 ± 0.12	0.08 ± 0.02	0.90 ± 0.09
GR	0.28 ± 0.03	0.32 ± 0.05	0.12 ± 0.04	0.60 ± 0.30	0.11 ± 0.02	0.60 ± 0.10

ACPD
15, 32831–32887, 2015

Figure 1. Stations where LIRIC algorithm was applied during ChArMEx/EMEP 2012 intensive measurement period on 9–11 July. Source: Google Earth.

ACPD
15, 32831–32887, 2015

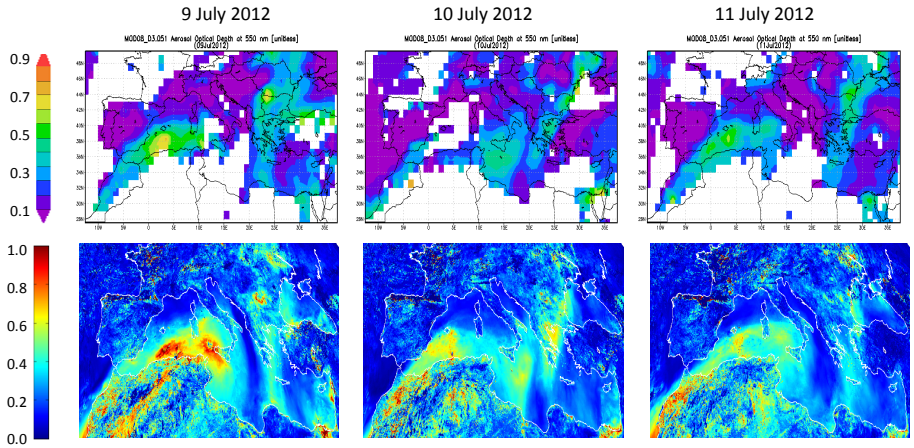

Figure 2. $\tau_{550\,nm}$ from MODIS/Terra (top) and $\tau_{675\,nm}$ daytime mean from MSG-SEVIRI (bottom) on 9, 10 and 11 July.

ACPD
15, 32831–32887, 2015

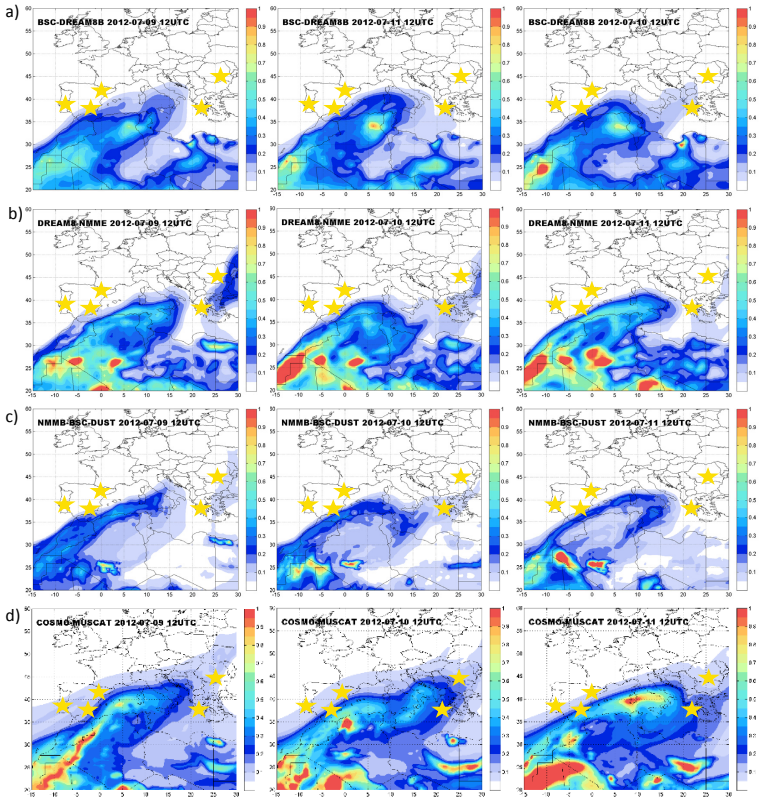

Figure 3. $\tau_{550\,nm}$ forecast by **(a)** BSC-DREAM8b, **(b)** DREAM8-NMME **(c)** NMMB/BSC-Dust and **(d)** COSMO-MUSCAT models for 9, 10 and 11 July 2012 at 12:00 UTC over Europe and North Africa. The yellow stars represent the location of the stations where microphysical properties profiles were retrieved with LIRIC.

ACPD
15, 32831–32887, 2015

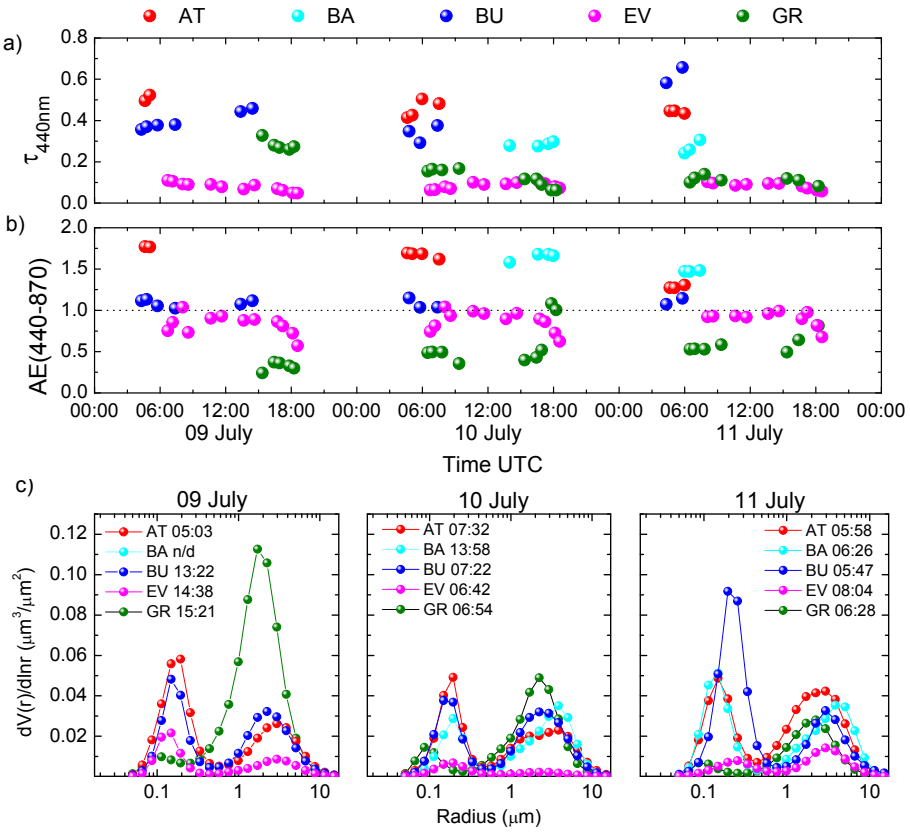

Figure 4. (a) AERONET Level 1.5 retrieved $\tau_{440\,nm}$ and **(b)** AE(440–870 nm) during CHARMEX 2012 campaign at the five stations (see Table 1 for station descriptions). **(c)** AERONET Version 2 Level 1.5 size distributions retrieved for 9, 10 and 11 July. n/d indicates no data availability.

ACPD
15, 32831–32887, 2015

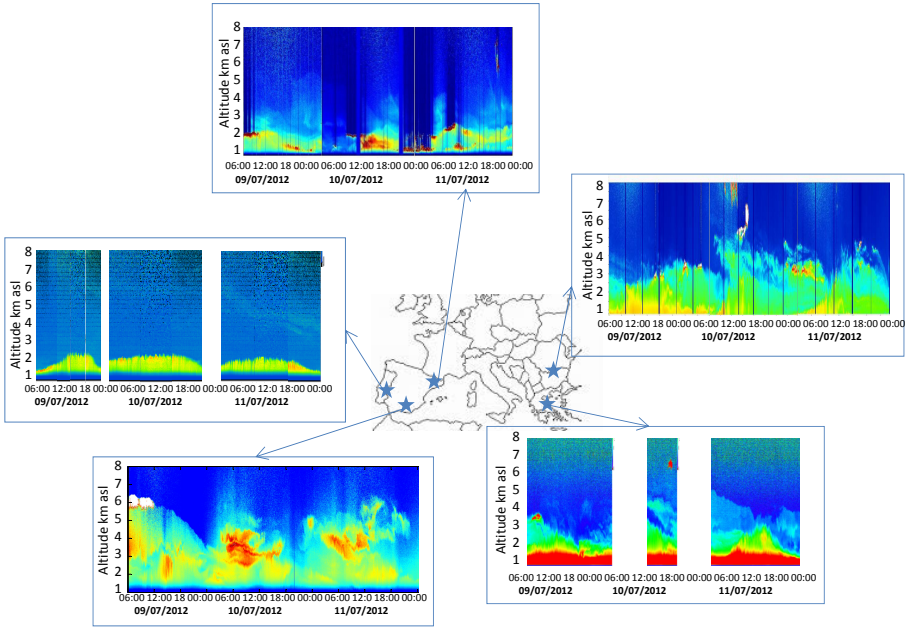

Figure 5. RCS at 532 nm (1064 nm at Athens) in arbitrary units for the five stations during ChArMEx 2012 measurements campaign.

ACPD
15, 32831–32887, 2015

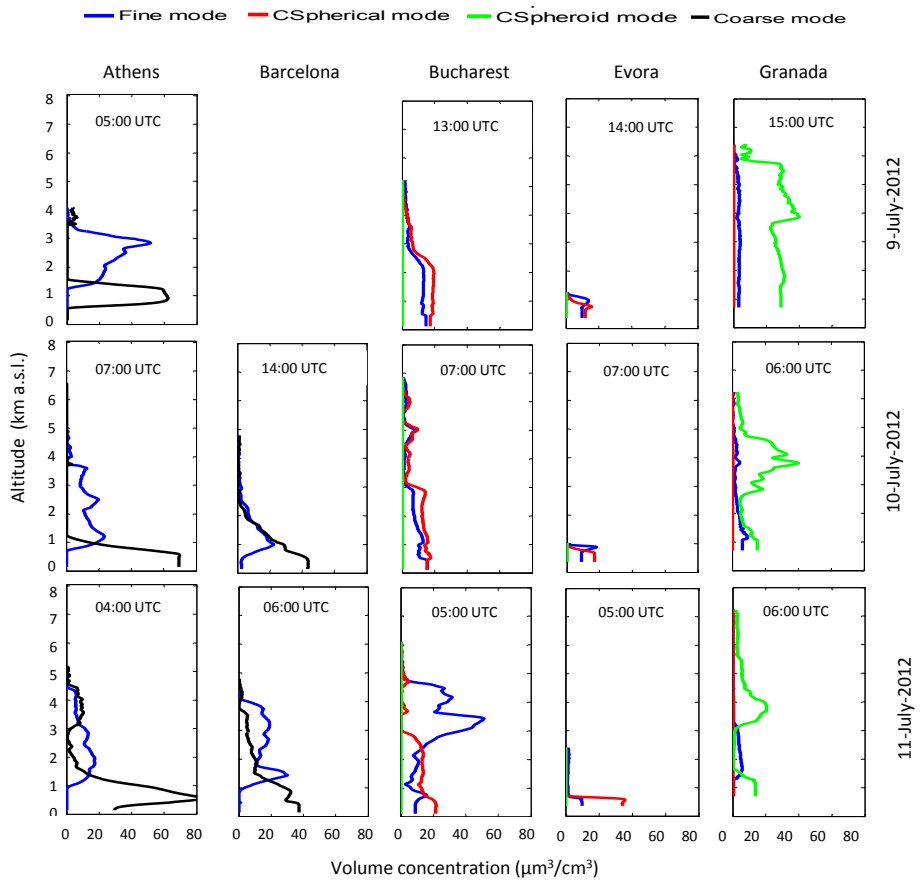

Figure 6. Volume concentration profiles of the total coarse mode and the fine mode at Barcelona and Athens, and volume concentration profiles of fine, coarse spherical and coarse spheroid mode at Évora, Bucharest and Granada (from left to right) for different periods of the 9, 10 and 11 July 2012 (from top to bottom).

ACPD
15, 32831–32887, 2015

Figure 7. MODIS FIRMS image indicating the active fires during the five previous days to 11 July 2012. The red line correspond to the air-mass 5 day back-trajectory arriving over Bucharest at 3000 m a.s.l. on 11 July 2012.

ACPD
15, 32831–32887, 2015

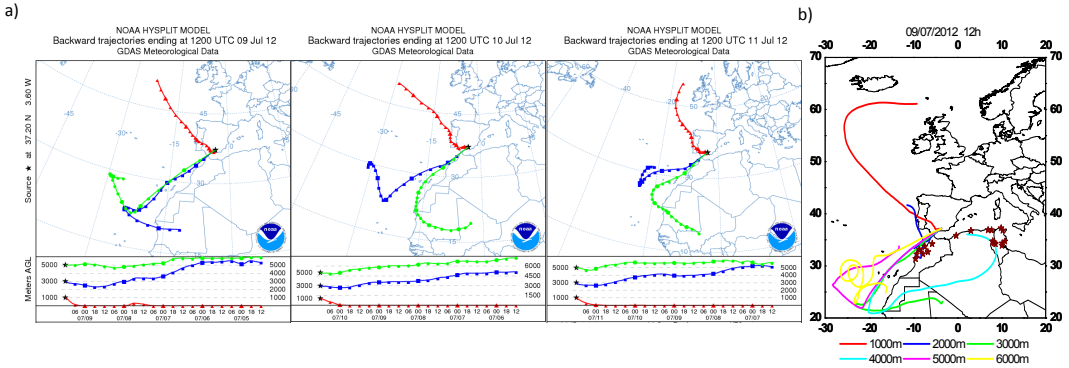

Figure 8. (a) 5 day backward trajectories arriving over Granada on 9, 10 and 11 July 2012 at 12:00 UTC (from left to right) computed by HYSPLIT model. **(b)** Locations of the main industrial activity in the North of Africa (brown stars)taken from Rodriguez et al. (2011) together with the 5 day backwards trajectories arriving at Granada experimental site on 9 July 2012 at 12:00 UTC.

ACPD
15, 32831–32887, 2015

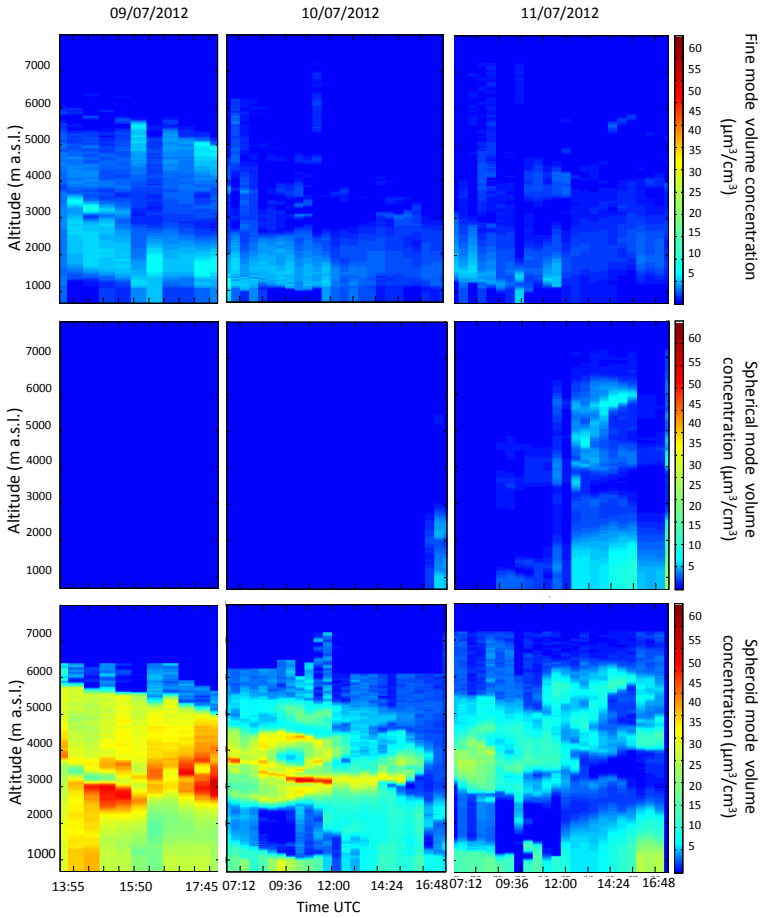

Figure 9. Time series of the volume concentration profiles (in $\mu m^3 cm^{-3}$) for the fine mode (upper part), coarse spherical mode (middle part) and coarse spheroid mode (lower part) for days 9, 10 and 11 July 2012 (from left to right).

ACPD
15, 32831–32887, 2015

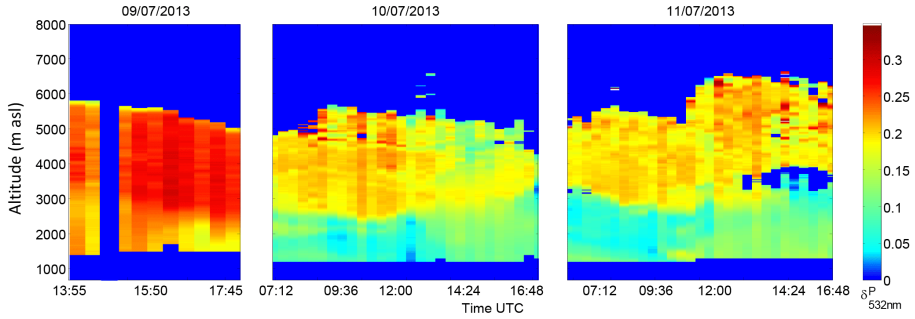

Figure 10. Time series of the $\delta^{P}_{532\,nm}$ profiles retrieved from Granada lidar system at different time intervals during during ChArMEx July 2012 intensive measurement period. Dark blue color represents regions and time periods where no data were retrieved.

ACPD
15, 32831–32887, 2015

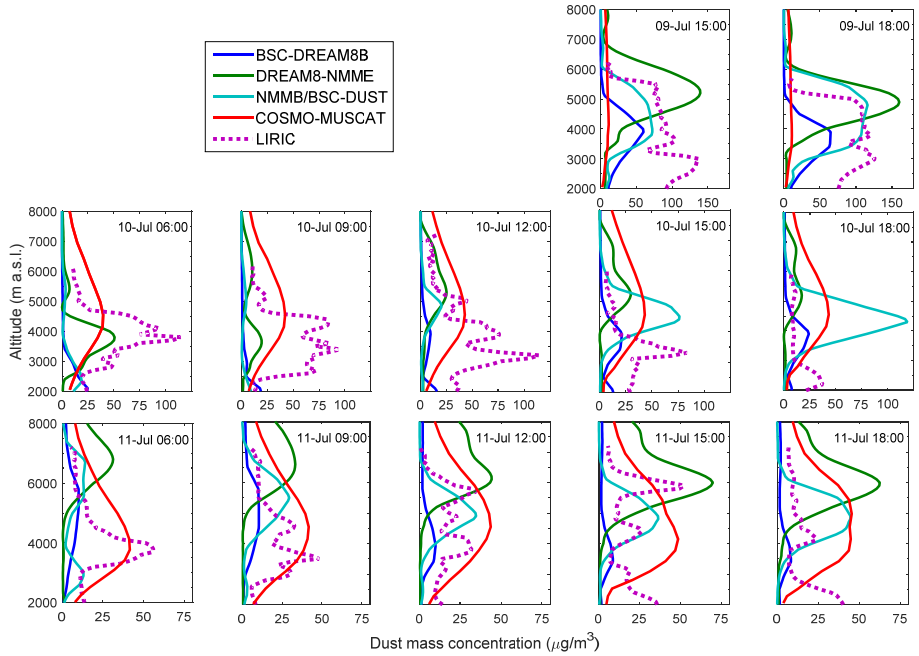

Figure 11. Dust mass concentration profiles obtained with LIRIC (dotted line) and BSC-DREAM8b-v2, DREAM8-NMME, DREAMABOL, NMMB/BSC-Dust for Granada station every three hours on 9, 10 and 11 July 2012.

ACPD
15, 32831–32887, 2015

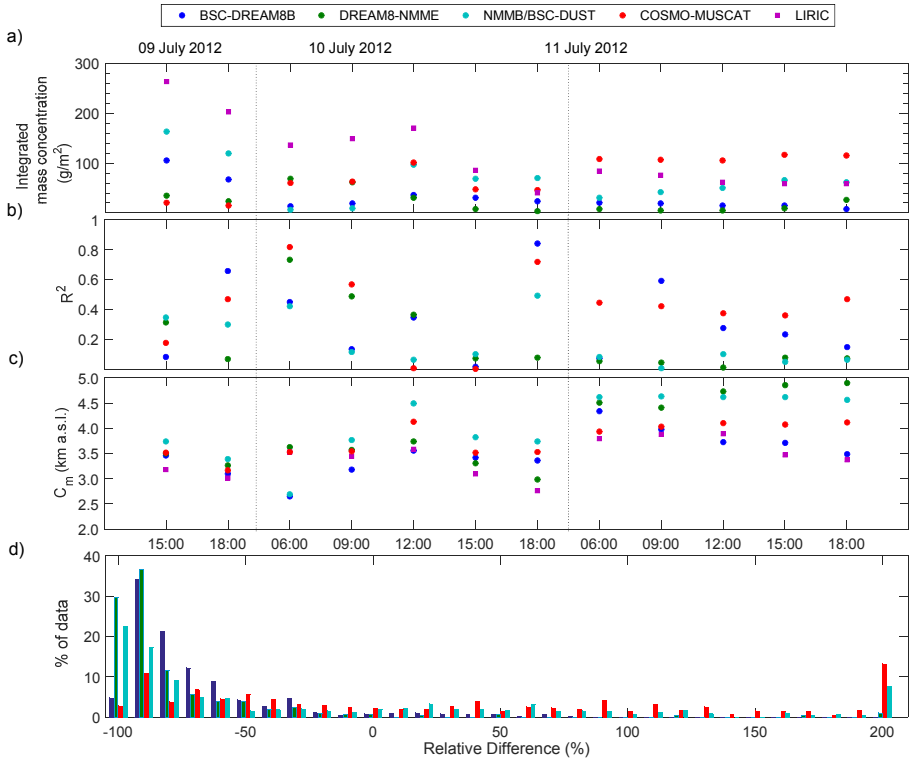

Figure 12. (a) Time series of the integrated mass concentration values (above 2 km in altitude) retrieved from LIRIC and the four evaluated models vertical profiles for the period between 15:00 UTC on 9 July 2012 and 18:00 UTC on 11 July 2012. **(b)** Time series of the determination coefficient, R^2 between LIRIC-derived mass concentration profiles and each one of the four evaluated models for the same period. **(c)** Time series of the dust center of mass, C_m obtained from LIRIC and the models profiles. **(d)** Histogram of the relative differences between LIRIC and the analysed models.

ACPD
15, 32831–32887, 2015

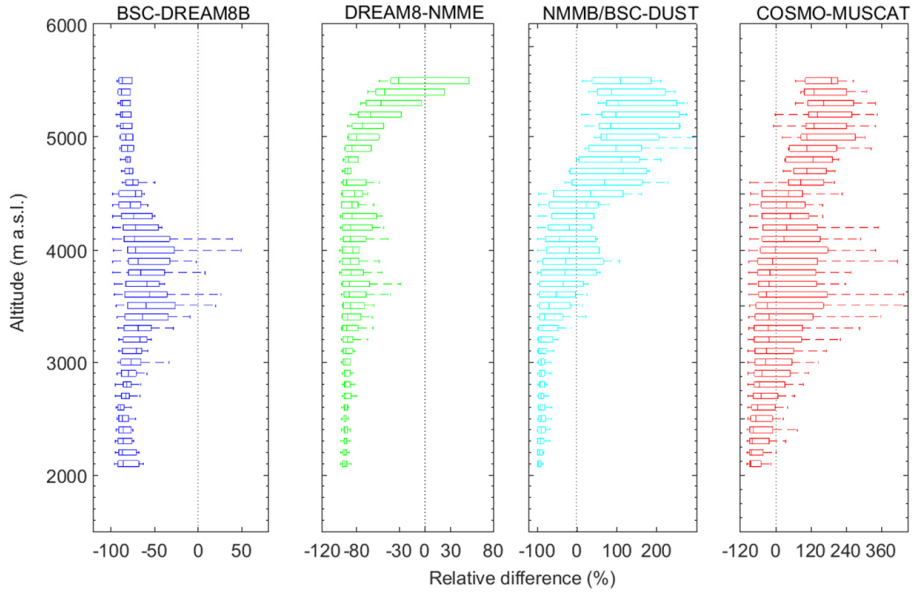

Figure 13. Box-whisker plots of the relative differences between LIRIC and the models distributed in 100 m layers for the dust mass concentration. The limits of the box represent the 10 and 90 percentiles, the central line is the median and the horizontal bars the standard deviation. Note the *x* axis changes with the model.

ACPD
15, 32831–32887, 2015